[redacted]

Copy No. 6

RM No. A8F15

NACA RM No. A8F15

UNCLASSIFIED

CLASSIFICATION CHANGED OCT 18 1948

[redacted]

NACA

naca Release form #582
authority of H. L. Dryden Date June 27, 1951
by HJR, 7-20-51

RESEARCH MEMORANDUM

INVESTIGATION OF A THIN WING OF ASPECT RATIO 4 IN THE AMES 12-FOOT PRESSURE WIND TUNNEL. II - THE EFFECT OF CONSTANT-CHORD LEADING- AND TRAILING-EDGE FLAPS ON THE LOW-SPEED CHARACTERISTICS OF THE WING

By Ben. H. Johnson, Jr., and Angelo Bandettini

Ames Aeronautical Laboratory
Moffett Field, Calif.

CLASSIFICATION CANCELLED

CLASSIFIED DOCUMENT

This document contains classified information affecting the National Defense of the United States within the meaning of the Espionage Act, USC 50:31 and 32. Its transmission or the revelation of its contents in any manner to an unauthorized person is prohibited by law. Information so classified may be imparted only to persons in the military and naval services of the United States, appropriate civilian officers and employees of the Federal Government who have a legitimate interest therein, and to United States citizens of known loyalty and discretion who of necessity must be informed thereof.

By J. W. Crowley Date 12/14/53
E.O. 10501
MHA 1/27/54 See naca
R7 1957

NATIONAL ADVISORY COMMITTEE FOR AERONAUTICS

WASHINGTON
October 18, 1948

UNCLASSIFIED

NACA LIBRARY
LANGLEY MEMORIAL AERONAUTICAL LABORATORY
Langley Field, Va.

[redacted]

3 1176 01331 5511

RESTRICTED

UNCLASSIFIED

[redacted]

NATIONAL ADVISORY COMMITTEE FOR AERONAUTICS

RESEARCH MEMORANDUM

INVESTIGATION OF A THIN WING OF ASPECT RATIO 4 IN THE AMES 12-FOOT PRESSURE WIND TUNNEL. II – THE EFFECT OF CONSTANT-CHORD LEADING- AND TRAILING-EDGE FLAPS ON THE LOW-SPEED CHARACTERISTICS OF THE WING

By Ben H. Johnson, Jr., and Angelo Bandettini

SUMMARY

Wind-tunnel tests have been made of a semispan model of an unswept wing of aspect ratio 4 and a taper ratio of 0.50, equipped with leading- and trailing-edge flaps. The basic airfoil profile was a diamond having a maximum thickness of 4.5 percent of the chord. The 50-percent-chord line of the wing was normal to the plane of symmetry. The purpose of the tests was to determine the low-speed aerodynamic characteristics of the wing as affected by the separate or combined deflections of a full-span, constant-chord, leading-edge, plain flap and a partial-span, constant-chord, trailing-edge flap of either the plain or split type.

Lift, drag, and pitching-moment data at a Mach number of 0.30 and a Reynolds number of 3,000,000 are presented for leading- and trailing-edge flaps deflected separately and in combination. The maximum lift coefficients obtained on the wing were as follows:

1.45 with the trailing-edge split flap and the leading-edge flap deflected

1.39 with the trailing-edge plain flap and the leading-edge flap deflected

1.26 with the trailing-edge split flap deflected

1.16 with the trailing-edge plain flap deflected

1.04 with the leading-edge flap deflected

0.74 with all flaps neutral (plain wing)

[redacted]

UNCLASSIFIED

The leading-edge flap was particularly effective in improving the pitching-moment characteristics of the wing, whether the flap was deflected alone or in combination with either of the trailing-edge flaps. Any of the flaps were effective in improving the lift-drag ratio at the higher lift coefficients.

The effects of scale and modification of the diamond profile by rounding the ridges were also investigated for a combination of plain leading- and trailing-edge flaps, optimum for maximum lift. The wing characteristics were little affected by profile modification or variation of the Reynolds number.

INTRODUCTION

For supersonic aircraft, the wings of which are not swept behind the Mach cone, airfoil sections with sharp leading edges are considered necessary to minimize the drag due to wave resistance. The maximum lift of such a wing profile at subsonic speeds is relatively low due to the occurrence of laminar separation at the wing leading edge at small angles of attack. Accordingly, auxiliary lift-producing devices are essential to provide the aircraft with acceptable landing and take-off characteristics.

In order to ascertain the effectiveness of constant-chord leading- and trailing-edge flaps applied to such a wing, tests of a semispan model have been conducted in the Ames 12-foot pressure wind tunnel. The model represented a wing of aspect ratio 4, a taper ratio of 0.50, with a sharp-edge diamond profile of thickness ratio 0.045. The tests were made at Mach numbers of 0.20 and 0.30 and at a range of Reynolds numbers from 3,000,000 to 10,000,000.

SYMBOLS

The following symbols are used in this report:

C_L lift coefficient $\left(\frac{\text{lift}}{qS}\right)$

C_D drag coefficient $\left(\frac{\text{drag}}{qS}\right)$

C_m pitching-moment coefficient about quarter-chord point of the wing mean aerodynamic chord $\left(\frac{\text{pitching moment}}{qSc'}\right)$

$C_{L_{max}}$ maximum lift coefficient

$\Delta C_{L_{max}}$ increment of maximum lift coefficient due to flap deflection

α angle of attack of wing-chord plane, degrees

$\alpha_{C_{L_{max}}}$ angle of attack at maximum lift

δ_n leading-edge flap deflection, positive downward, degrees

δ_f trailing-edge plain-flap deflection, positive downward, degrees

δ_{sf} trailing-edge split-flap deflection, positive downward, degrees

M Mach number $\left(\frac{V}{a}\right)$

R Reynolds number $\left(\frac{\rho V c'}{\mu}\right)$

where

S area of the semispan wing, square feet

c' wing mean aerodynamic chord, chord through centroid of area of wing semispan plan form, feet

c local chord, feet

q free-stream dynamic pressure $(\frac{1}{2}\rho V^2)$, pounds per square foot

ρ mass density of air, slugs per cubic foot

V airspeed, feet per second

μ viscosity of air, slugs per foot-second

a speed of sound, feet per second

MODEL AND APPARATUS

The tests were conducted in the Ames 12-foot wind tunnel which is a closed-throat, variable-density wind tunnel with a low turbulence

level, closely approximating that of free air. A description of the tunnel will be found in reference 1.

The semispan model used in this investigation was the same as that used in the tests reported in reference 1. The effective geometric aspect ratio was 4 and the taper ratio was 0.50. The 50-percent-chord line of the wing was normal to the free stream. The initial wing profile was a diamond section having a thickness ratio of 0.045. Subsequent modification by rounding of the ridges resulted in a thickness ratio of 0.042.

The wing was fitted with a full-span, constant-chord, leading-edge, plain flap and with a partial-span, constant-chord, trailing-edge flap of either the split or plain type. The dimensions of the wing are shown in figure 1. The area of the leading-edge flap was 15 percent of the total wing area and that of the trailing-edge flaps was 12 percent. The two trailing-edge flaps were geometrically similar in plan form. The unsealed gap between the plain flaps and the wing was 0.015 inch with the flaps undeflected.

The model was constructed of solid steel and was mounted in the tunnel as shown in figure 2. The plain flaps were hinged and were held rigidly at given deflections by steel angle plates. The split flap was held in position on the wing by wooden blocks as shown in figure 2. The deflection of the flaps under aerodynamic loads was negligible.

CORRECTIONS TO DATA

The data have been corrected for effects of tunnel-wall interference and model-support tare forces. Because of the small size of the model and the low Mach numbers, corrections for constriction due to the tunnel walls were negligible.

The data have been corrected for tunnel-wall interference by the method of reference 2. The following corrections were added:

$$\Delta\alpha = 0.363\ C_L$$

$$\Delta C_D = 0.0056\ C_L^2$$

$$\Delta C_m = 0$$

Tare corrections due to air forces exerted on the exposed area of the turntable were obtained from force measurements made with the

model removed from the tunnel. Possible interference effects between the model and the turntable were not evaluated but they are believed to be small. The magnitude of the measured tare drag varied with Reynolds number and had the following values based on the wing area:

Reynolds number	C_D Tare
2,000,000	0.0063
3,000,000	.0059
6,000,000	.0057
10,000,000	.0056

TESTS

Lift, drag, and pitching-moment data were obtained as a function of the angle of attack for both wing profiles. Data were obtained at a Mach number of 0.30 and a Reynolds number of 3,000,000 for the flap deflections given in the table below:

Leading-edge flap deflection, δ_n (deg)	Trailing-edge plain-flap deflection, δ_f (deg) (1)	Trailing-edge split-flap deflection, δ_{sf} (deg) (2)
0	0, 20, 40, 50, 60	0, 40, 50, 60, 70
20	0 (round-ridge profile)	0
25	0, 50, 60	40, 50, 60
30	0, 50, 60	40, 50, 60
35	0, 50, 60	40, 50, 60, 70

[1]Sharp-ridge profile except as noted.
[2]Round-ridge profile.

Data were obtained on both the sharp-ridge and the round-ridge profile at a Mach number of 0.20 for a range of Reynolds numbers from 3,000,000 to 10,000,000 with a deflection of the leading-edge flap δ_n of 30° and a deflection of the trailing-edge plain flap δ_f of 50°.

RESULTS

The lift, drag, and pitching-moment characteristics of the wing as affected by individual deflections of the two types of trailing-edge flaps and of the leading-edge flap are presented in figures 3 to 5 and for various combinations of leading- and trailing-edge flap deflections in figures 6 and 7. These data were obtained at a Reynolds number of 3,000,000 and a Mach number of 0.30.

Figure 8 shows the effect of scale and the effect of rounding the wing ridges on the aerodynamic characteristics of the wing with the leading-edge flap and the trailing-edge plain flap deflected. These data were obtained at a Mach number of 0.20 and Reynolds numbers of 3,000,000, 6,000,000, and 10,000,000.

DISCUSSION

Maximum Lift Characteristics

The following table summarizes the test data pertaining to maximum lift characteristics at a Mach number of 0.30 and a Reynolds number of 3,000,000:

Model configuration	Flap angles (deg)	$C_{L_{max}}$	$\alpha_{C_{L_{max}}}$ (deg)	C_m at $C_{L_{max}}$	L/D at $C_{L_{max}}$
Plain wing (sharp-ridge profile)	- - - - - -	0.74	12.5	-0.10	4.3
Plain wing (round-ridge profile)	- - - - - -	0.74	13.0	-.09	4.3
Trailing-edge plain flap (sharp-ridge profile)	$\delta_f = 60$	1.16	9.0	-.20	4.0
Trailing-edge split flap (round-ridge profile)	$\delta_{sf} = 70$	1.26	9.9	-.23	3.6
Leading-edge plain flap (sharp-ridge profile)	$\delta_n = 25$	1.04	19.5	-.12	4.3
Leading-edge flap and trailing-edge plain flap (sharp-ridge profile)	$\delta_n = 30$ and $\delta_f = 50$	1.39	17	-.13	5.0
Leading-edge flap and trailing-edge plain flap (round-ridge profile)	$\delta_n = 30$ and $\delta_f = 50$	1.38	16.5	-.17	5.1
Leading-edge flap and trailing-edge split flap (round-ridge profile)	$\delta_n = 30$ and $\delta_{sf} = 60$	1.45	17	-.20	4.5

Of the various model configurations tested, the trailing-edge split flap in conjunction with the leading-edge flap produced the highest maximum lift. However, substitution of a plain flap for the split flap resulted in only slightly reduced maximum lift and somewhat improved the lift-drag ratio at maximum lift.

The increased lift-drag ratios with the leading-edge flap deflected is evidence of the effectiveness of the leading-edge

flap in delaying the flow separation which occurs as a result of the sharp leading-edge profile. The use of the leading-edge flap in conjunction with either of the trailing-edge flaps reduced the pitching moment at maximum lift and greatly increased the angle of attack of maximum lift.

The increment of maximum lift and the angle of attack for maximum lift as functions of flap angle with each of the three flaps deflected independently are presented in figure 9. These data show that the split flap produces as much as 25 percent greater increment of maximum lift than the plain flap. The angle of attack for maximum lift was also higher for the split flap than for the plain flap.

Pitching-Moment Characteristics

Flaps deflected independently.- Comparison of the pitching-moment data of figures 3 to 5 indicates the effects of deflections of the various flaps on the rearward movement of the aerodynamic center which, as noted in reference 1, started at an angle of attack of approximately 6° for the plain wing. While deflection of the trailing-edge flaps had only a small effect on the angle of attack at which this movement started, deflection of the leading-edge flap delayed the movement to very near maximum lift. (See, e.g., fig. 5(a).)

The data for the wing with the trailing-edge flaps deflected show that at zero lift there was a large aft movement of the center of pressure due to flap deflection, the largest portion of this movement occurring for flap deflections less than 40°.

Flaps deflected in combination.- A comparison of the pitching-moment data of figures 3 and 6 for the plain flap and those of figures 4 and 7 for the split flap shows that deflection of the leading-edge flap in combination with the deflection of the trailing-edge flap increases the lift coefficient at which the rearward movement of the aerodynamic center starts. This is further evidence of the effectiveness of the leading-edge flap in delaying the flow separation caused by the sharp leading edge.

Drag Coefficients

The drag data of figures 3, 4, and 5 indicate that the minimum

drag increases as the flaps are deflected. The rate of rise of drag with lift decreases with increasing flap deflection for both of the trailing-edge flaps. For the leading-edge flap, the rate of rise of drag with lift is decreased by flap deflection up to 25° but is little affected by deflection of the flap above 25°.

Lift-Drag Ratio

The lift-drag ratio as a function of lift coefficient for the wing with various deflections of the flaps is presented in figure 10. Figures 10(a) and 10(b) show the lift-drag ratio of the wing with the two types of trailing-edge flaps deflected. Deflection of the flaps caused a reduction in the maximum lift-drag ratio and a slight increase in the lift-drag ratio at the higher lift coefficients. Figure 10(c) shows the lift-drag ratio of the wing with the leading-edge flap deflected. With 20° of leading-edge flap deflection, the maximum lift-drag ratio was 17.7 percent above the value of 14.1 obtained with the plain wing. With the flap deflected 25° or more, the maximum lift-drag ratio was less than that of the plain wing. For all flap deflections, the lift coefficient for maximum lift-drag ratio increased with increasing flap angle. The lift-drag ratios of the wing with deflection of the leading-edge flap and the trailing-edge flap optimum for maximum lift are presented in figure 10(d).

The Effect of Reynolds Number and Profile Modification

The effect of Reynolds number on the lift, drag, and pitching-moment characteristics of the wing with the leading-edge flap deflected 30° and the trailing-edge plain flap deflected 50° is shown in figure 8. Data are shown for the wing with the basic diamond profile and also with the modified profile having round ridges. At a Reynolds number of 3,000,000, rounding the ridges resulted in a rearward shift of the aerodynamic center at high lift coefficients. For the wing with sharp ridges, increasing the Reynolds number from 3,000,000 to 6,000,000 results in a similar rearward movement of the aerodynamic center and also causes a slight reduction in drag. For the modified wing with round ridges, increasing Reynolds number had no effect other than to cause a slight reduction in the drag.

SUMMARY OF RESULTS

The following results were obtained from the tests of a thin unswept wing equipped with constant-chord leading- and trailing-edge flaps:

1. The optimum flap angles for maximum lift and the corresponding values of maximum lift coefficient were as follows:

Leading-edge plain-flap deflection (deg)	Trailing-edge plain-flap deflection (deg)	Trailing-edge split-flap deflection (deg)	Maximum lift coefficient
0	0	0	0.74
0	60	---	1.16
0	---	70	1.26
25	0	0	1.04
30	50	---	1.39
30	---	60	1.45

2. The leading-edge flap, whether used independently or in conjunction with a trailing-edge flap, had a favorable influence on the pitching-moment characteristics of the wing. Deflection of this flap delayed the flow separation caused by the sharp leading edge as evidenced by the higher lift coefficients at which the center of lift on the wing moved rearward.

3. The maximum lift-drag ratio was improved 17.7 percent over the value of 14.1 for the plain wing by deflection of the leading-edge flap. Deflection of either of the trailing-edge flaps for the range of flap angles tested reduced the maximum lift-drag ratio but improved the lift-drag ratio at the higher lift coefficients. The lift-drag ratios at high lift coefficients were greater with the trailing-edge plain flap than with the trailing-edge split flap.

4. For the combinations of flap deflections tested, modification of the wing profile by rounding the ridges practically eliminated a small scale effect evident in the pitching-moment data at the higher lift coefficients. Variation of the Reynolds number from 3,000,000 to 10,000,000 had no effect upon the lift and only slightly reduced the drag.

Ames Aeronautical Laboratory,
National Advisory Committee for Aeronautics,
Moffett Field, Calif.

REFERENCES

1. Johnson, Ben H., Jr.: Investigation of a Thin Wing of Aspect Ratio 4 in the Ames 12-Foot Pressure Wind Tunnel. I – Characteristics of a Plain Wing. NACA RM No. A8D07, 1948.

2. Sivells, James C., and Deters, Owen J.: Jet Boundary and Plan Form Corrections for Partial-Span Models With Reflection Plane, End Plate, or no End Plate, in a Closed Circular Wind Tunnel. NACA TN No. 1077, 1946.

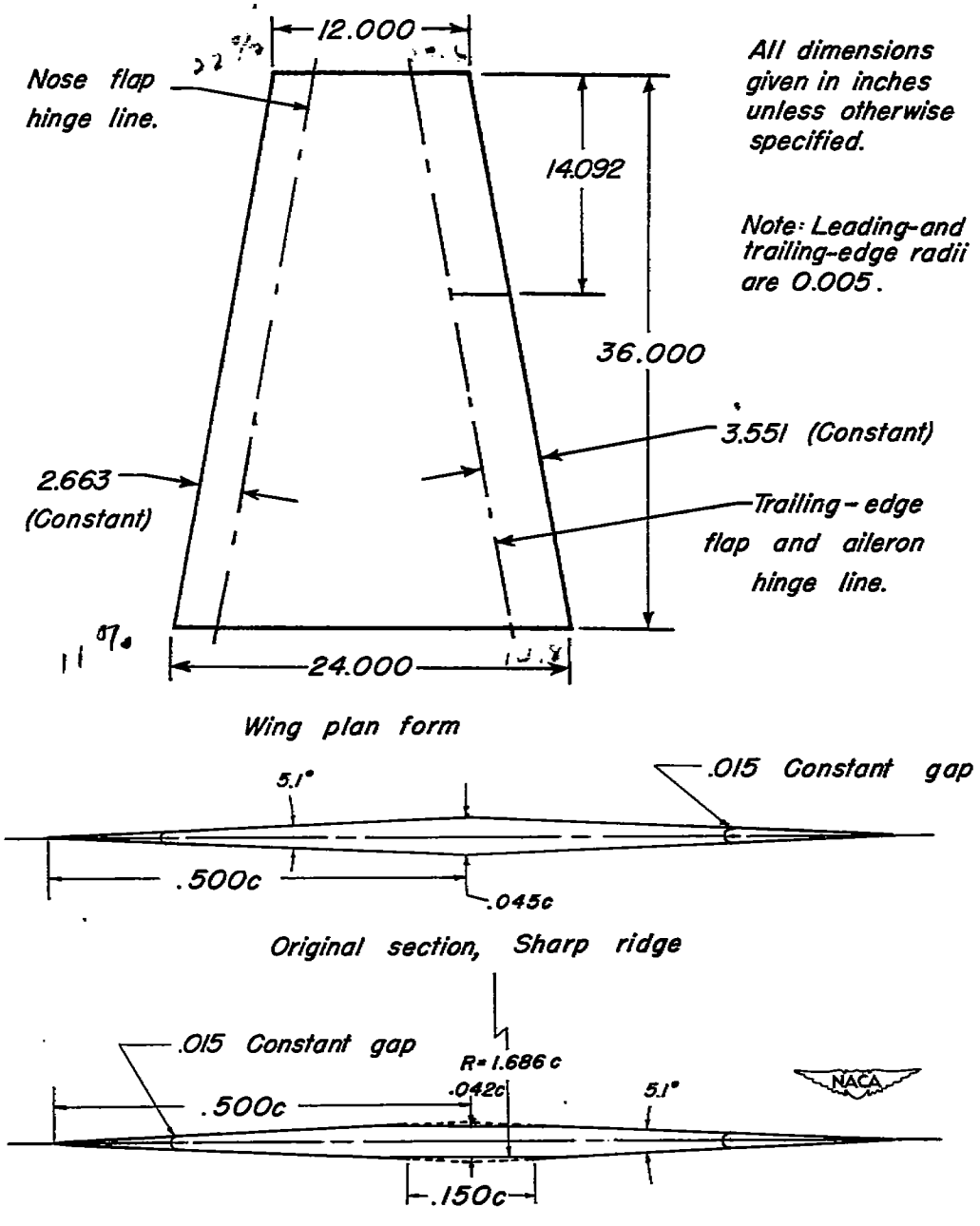

Figure 1.-Semispan model of a wing of aspect ratio 4, tested in the 12-foot pressure wind tunnel.

[redacted]

(a) Wing with the flaps undeflected.

(b) Wing with the leading-edge flap deflected 30° and the trailing-edge split flap deflected 60°.

Figure 2.- Semispan model of a wing of aspect ratio 4, mounted in the Ames 12-foot pressure wind tunnel.

[redacted]

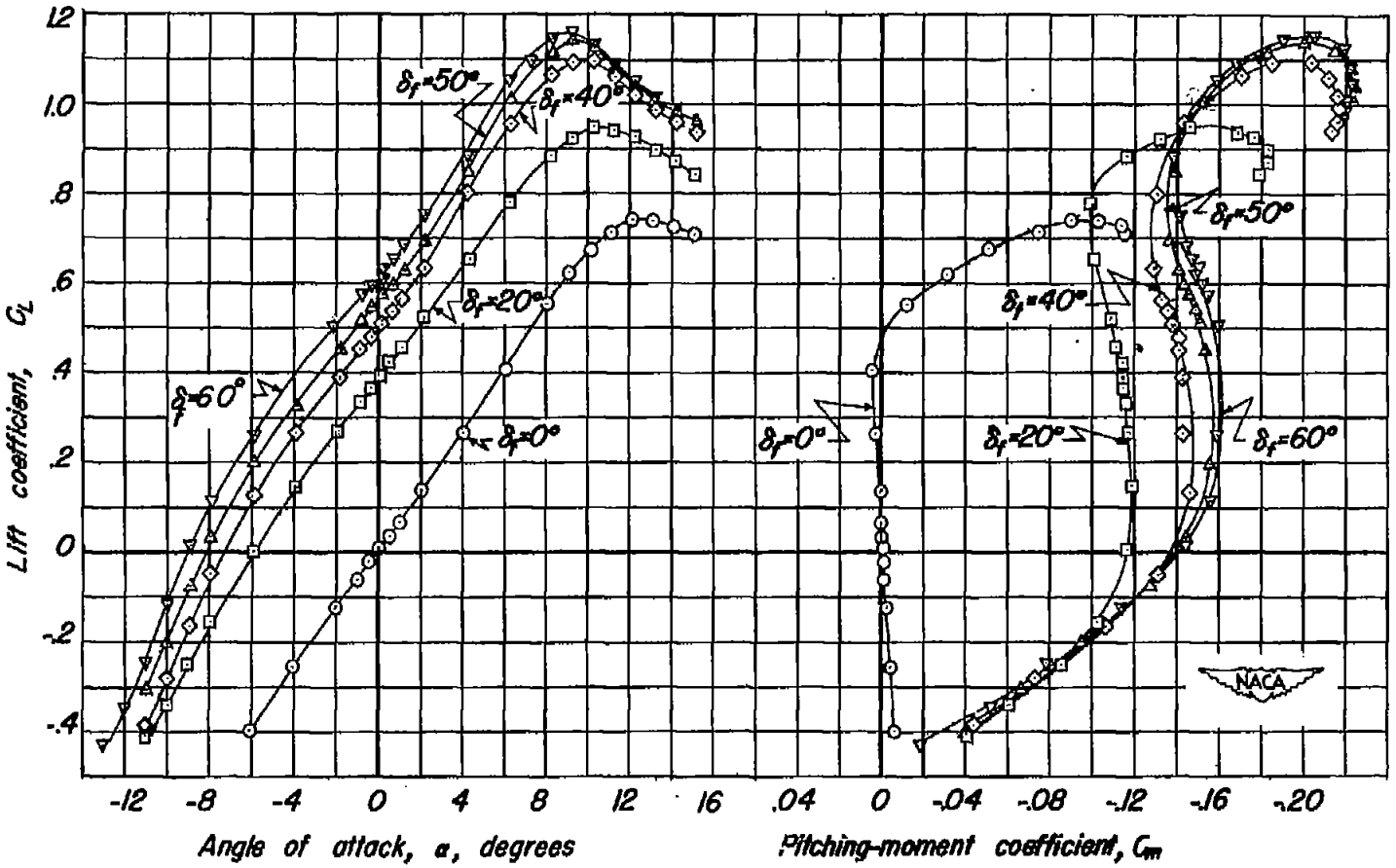

(a) C_L vs α, C_L vs C_m.

Figure 3.— The effect of the trailing-edge plain flap on the aerodynamic characteristics of the wing with the sharp-ridge profile. R, 3,000,000 , M, 0.30.

[redacted]

[redacted]

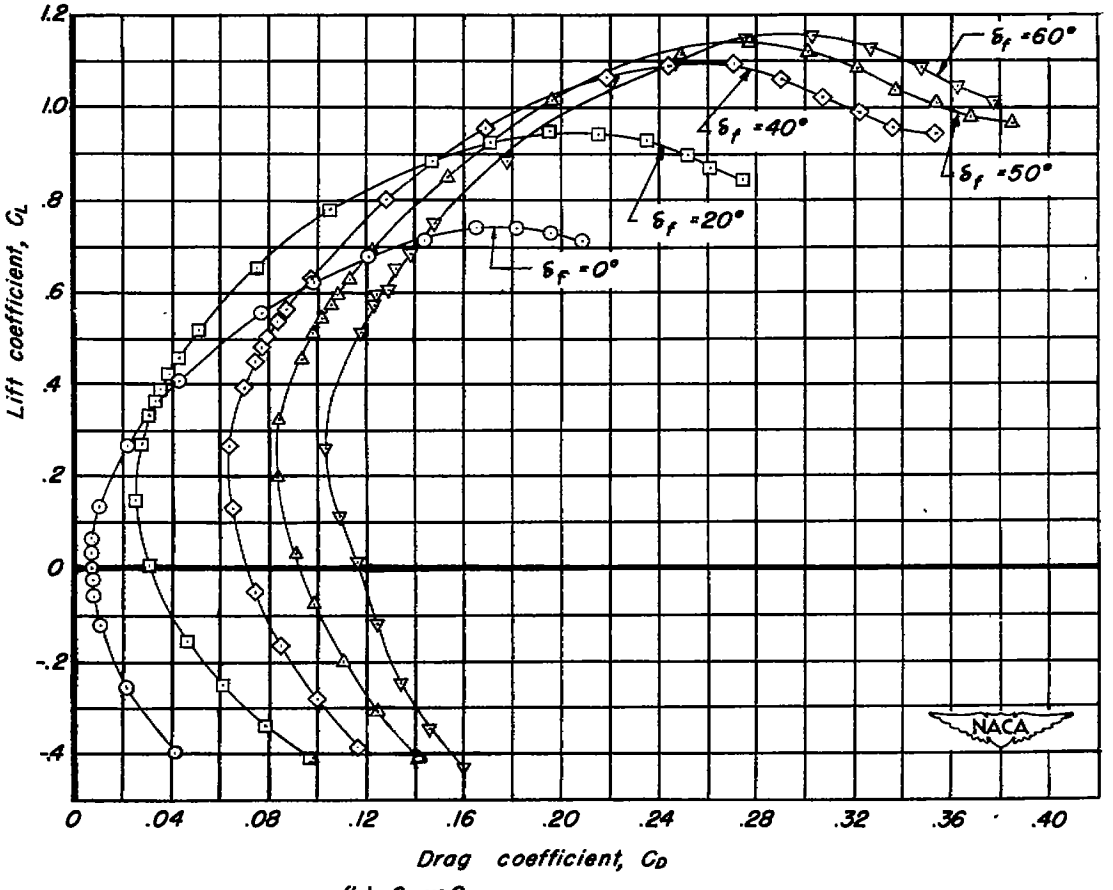

(b) C_L vs C_D.

Figure 3.– Concluded.

[redacted]

[redacted]

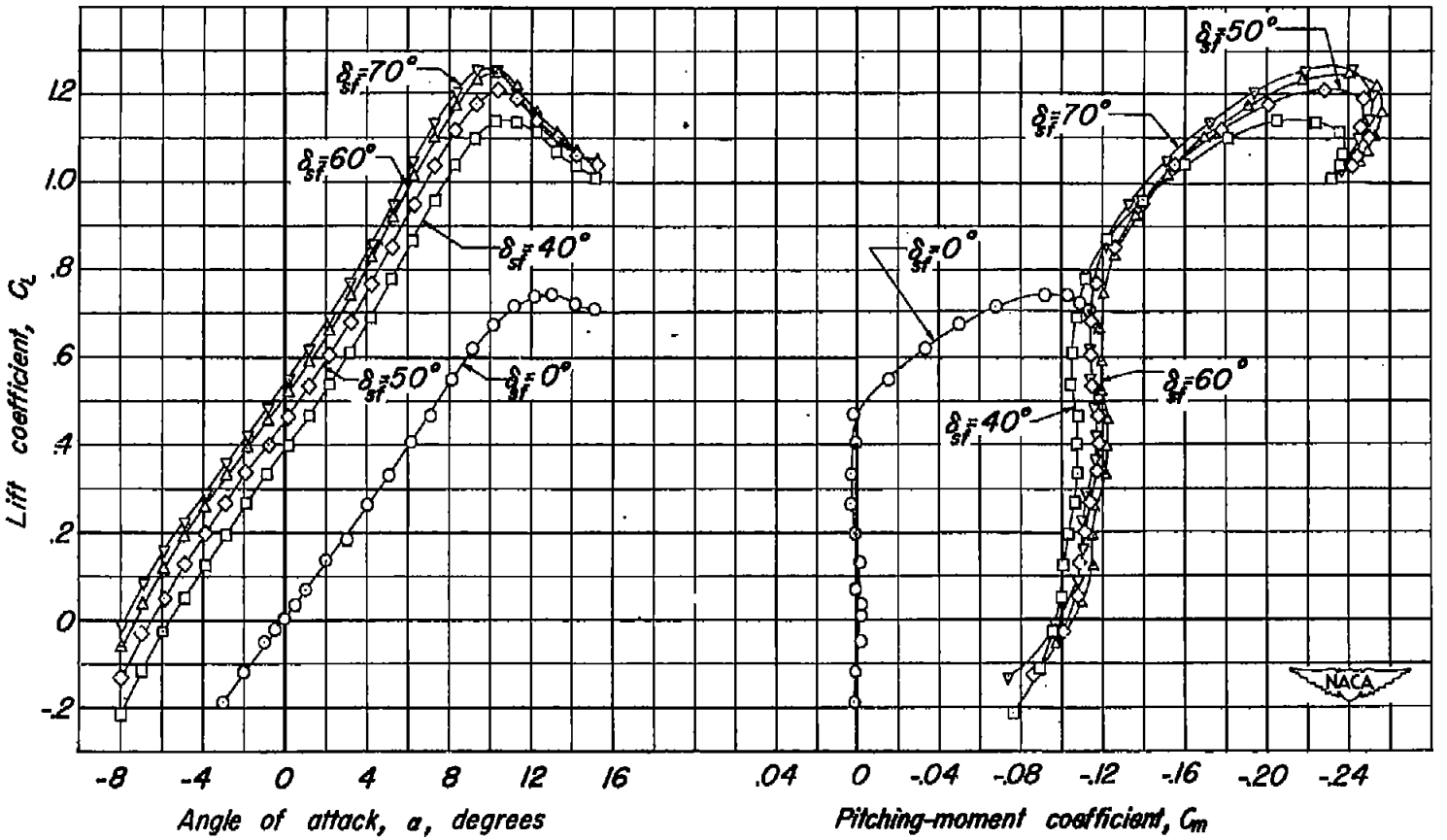

(a) C_L vs α, C_L vs C_m.

Figure 4.– The effect of the trailing-edge split flap on the aerodynamic characteristics of the wing with the round-ridge profile. R,3,000,000, M,0.30.

[redacted]

[redacted]

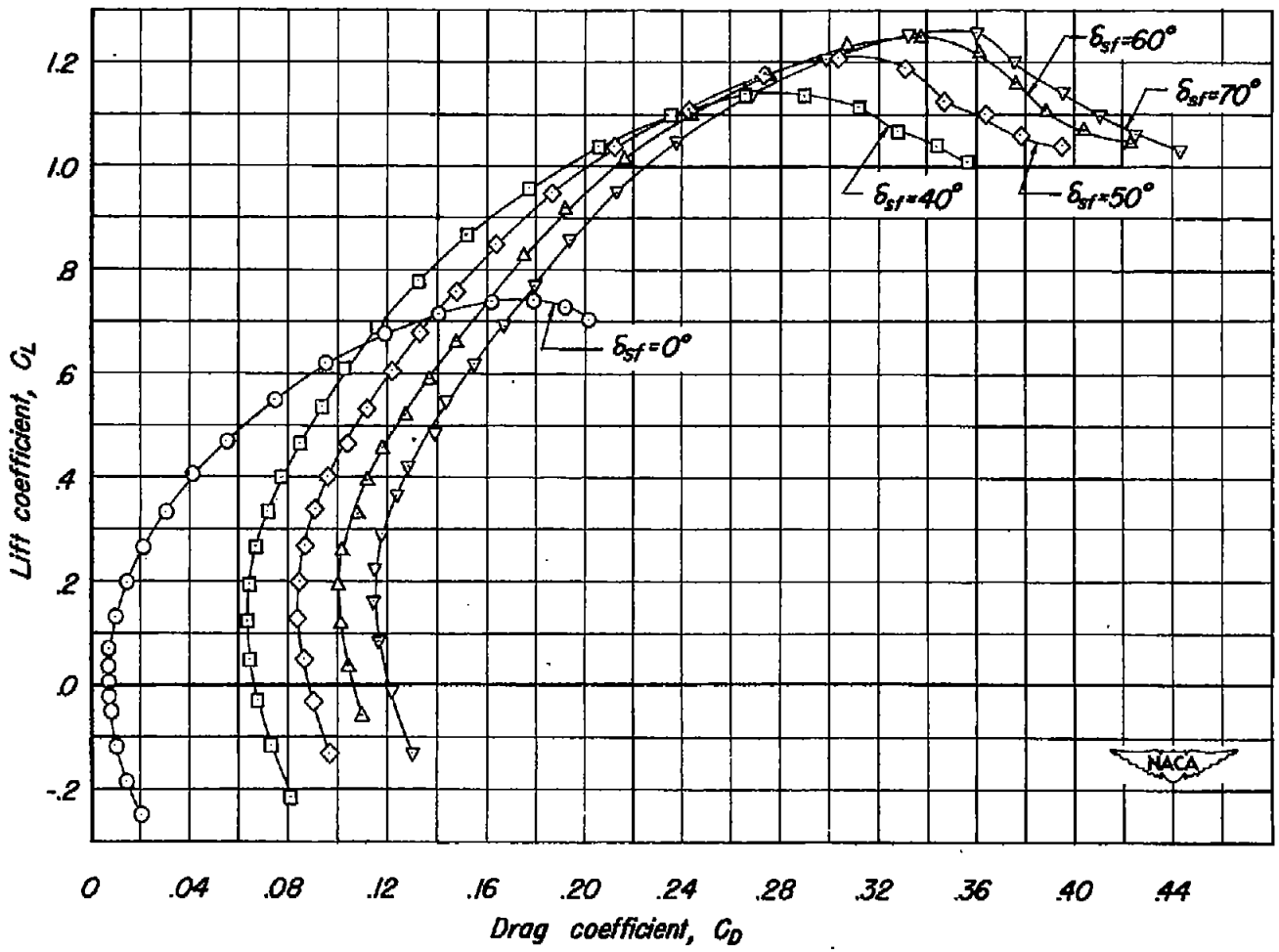

(b) C_L vs C_D.

Figure 4.—Concluded.

[redacted]

[redacted]

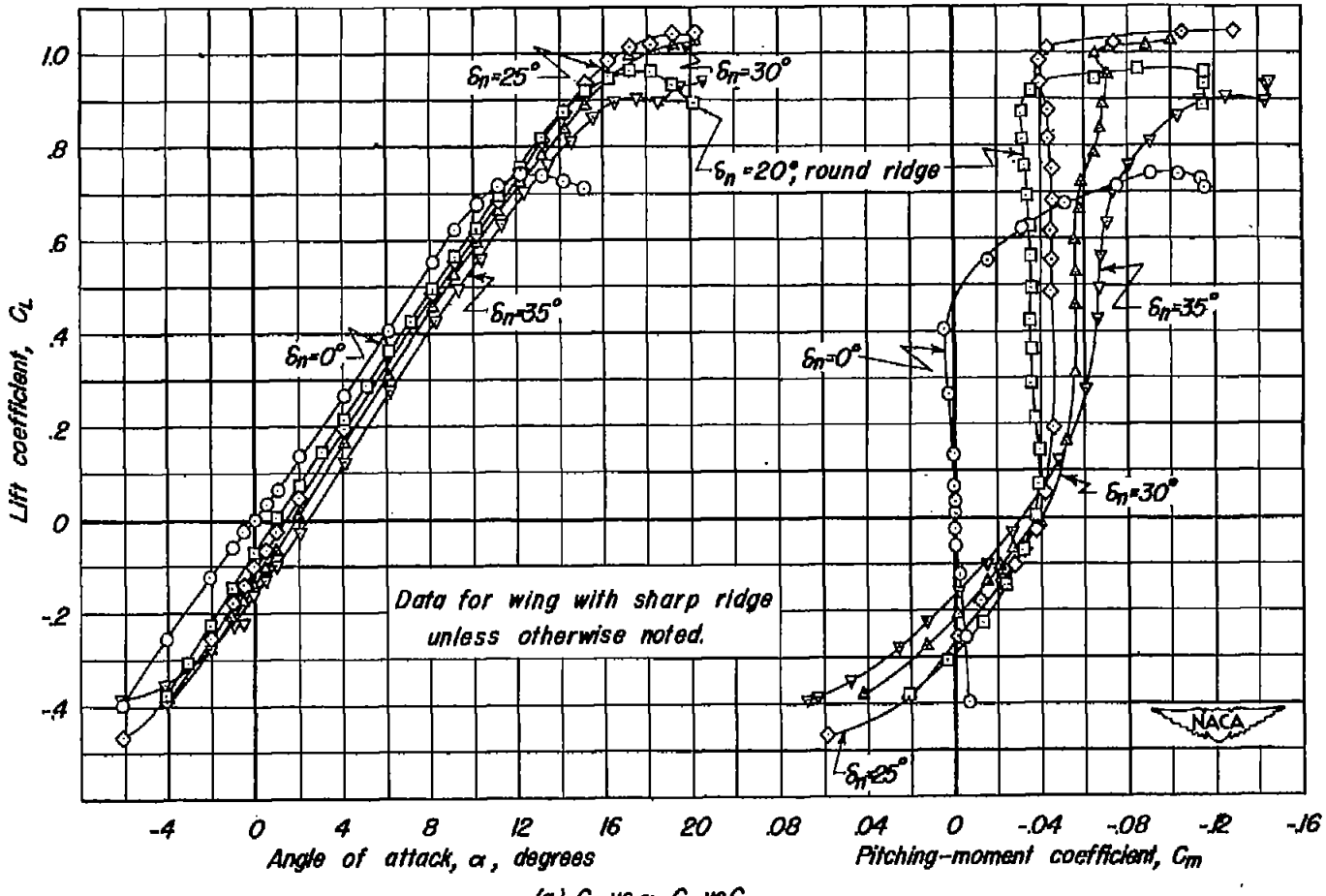

(a) C_L vs α, C_L vs C_m

Figure 5.—The effect of the leading-edge flap on the aerodynamic characteristics of the wing. R, 3,000,000; M, 0.30.

[redacted]

[redacted]

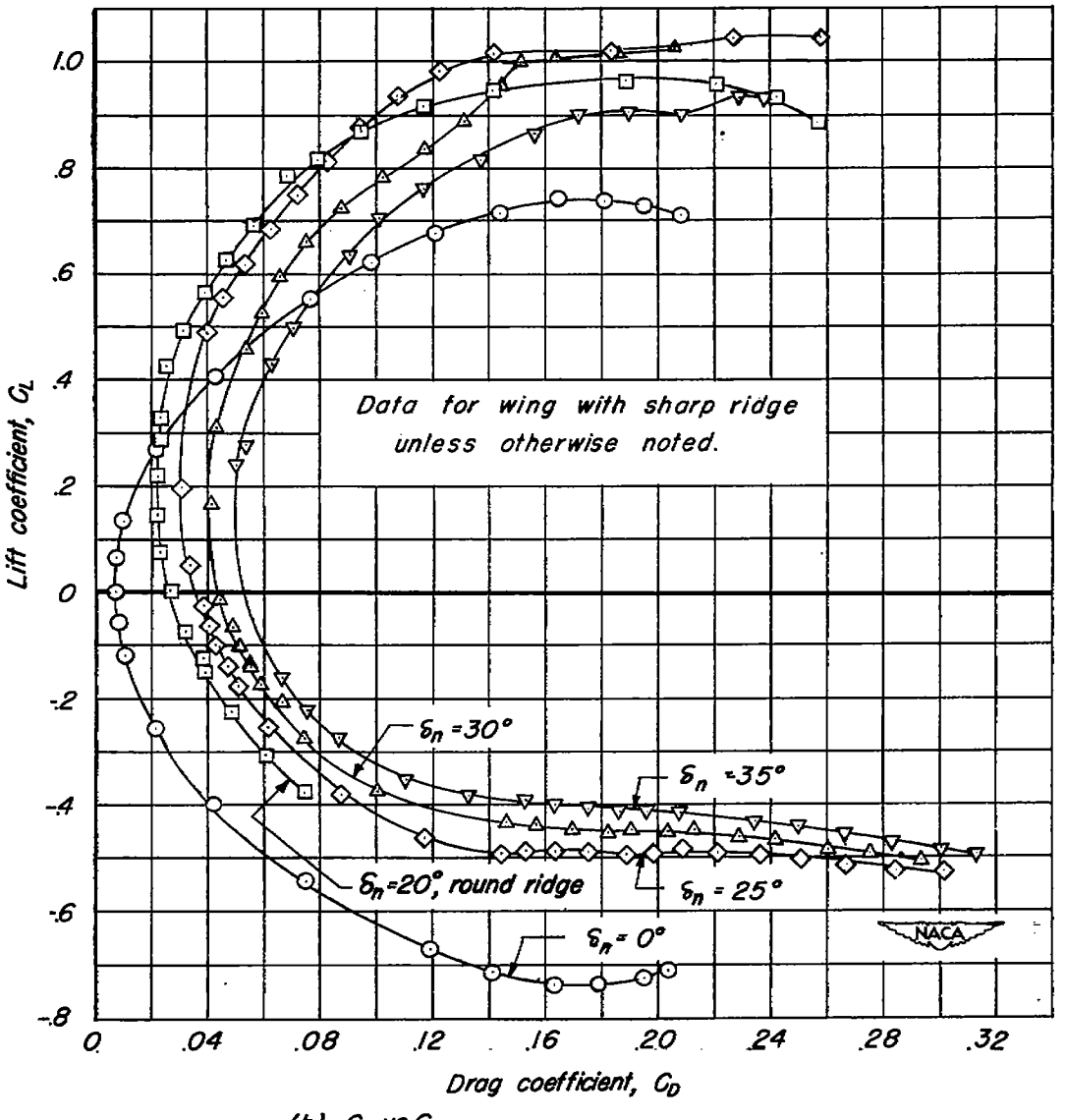

(b) C_L vs C_D.

Figure 5.— Concluded.

[redacted]

[redacted]

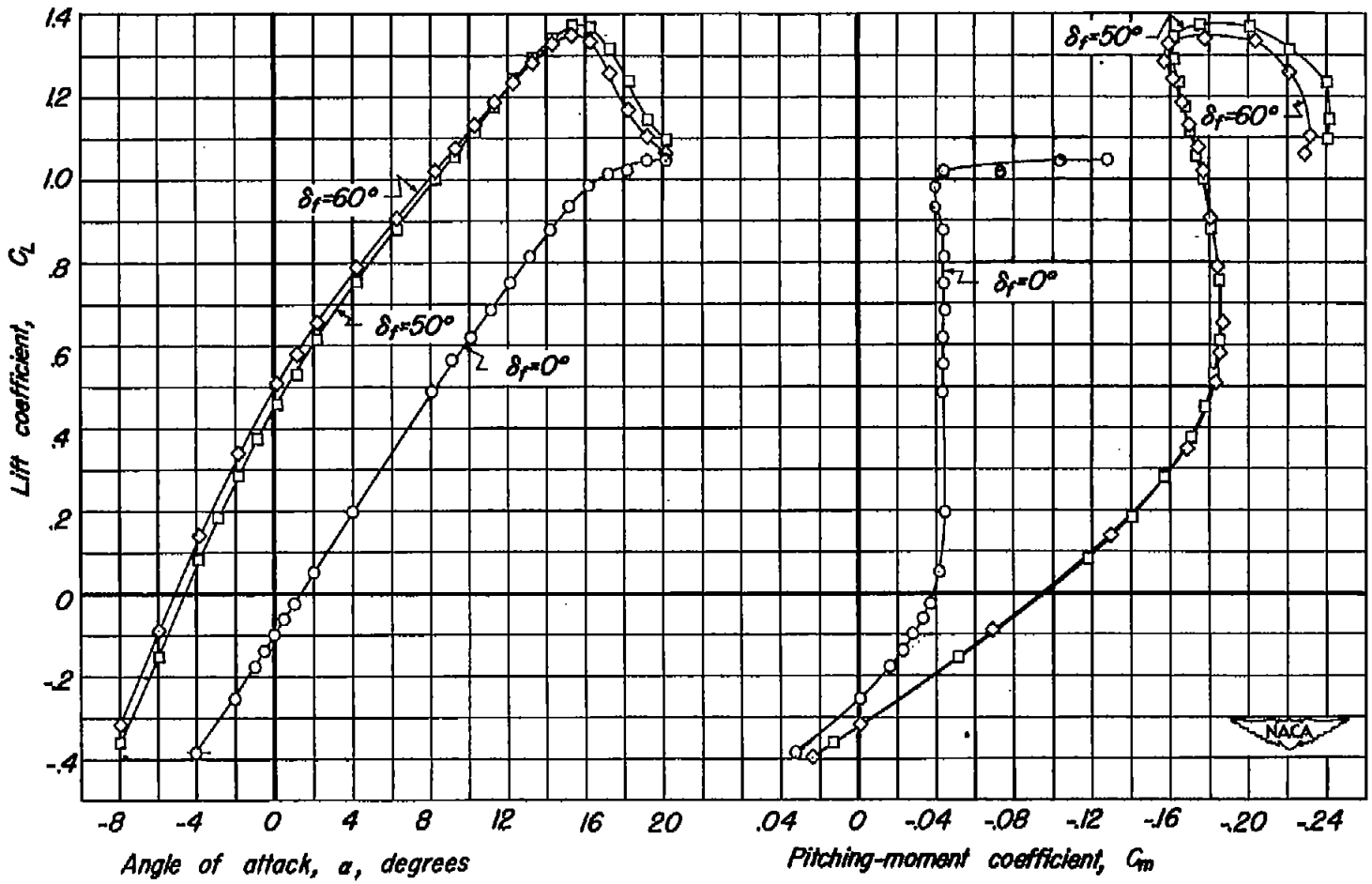

(a) C_L vs α, C_L vs C_m for δ_n=25°.

Figure 6.—The effect of the combination of the leading-edge flap and the trailing-edge plain flap on the aerodynamic characteristics of the wing with the sharp ridge. R,3,000,000;M,0.30.

[redacted]

[redacted]

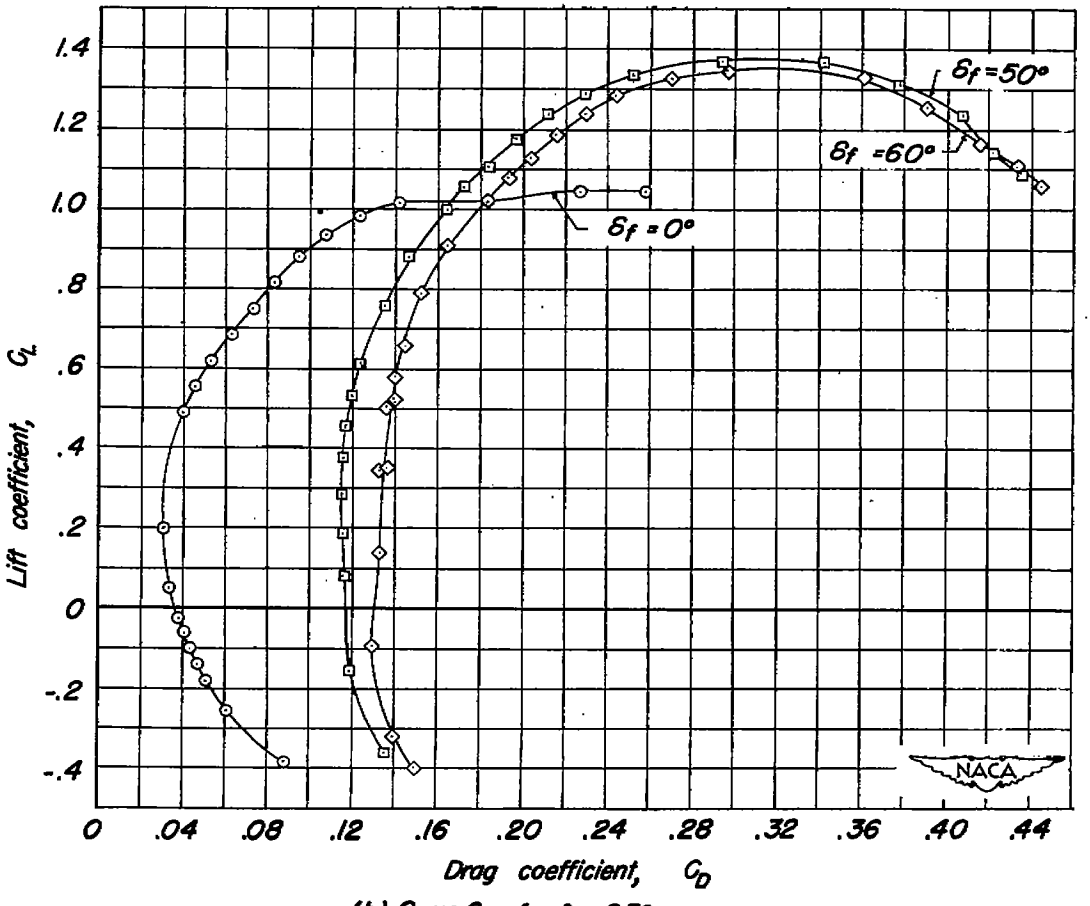

(b) C_L vs C_D for $\delta_n = 25°$

Figure 6.– Continued.

[redacted]

[redacted]

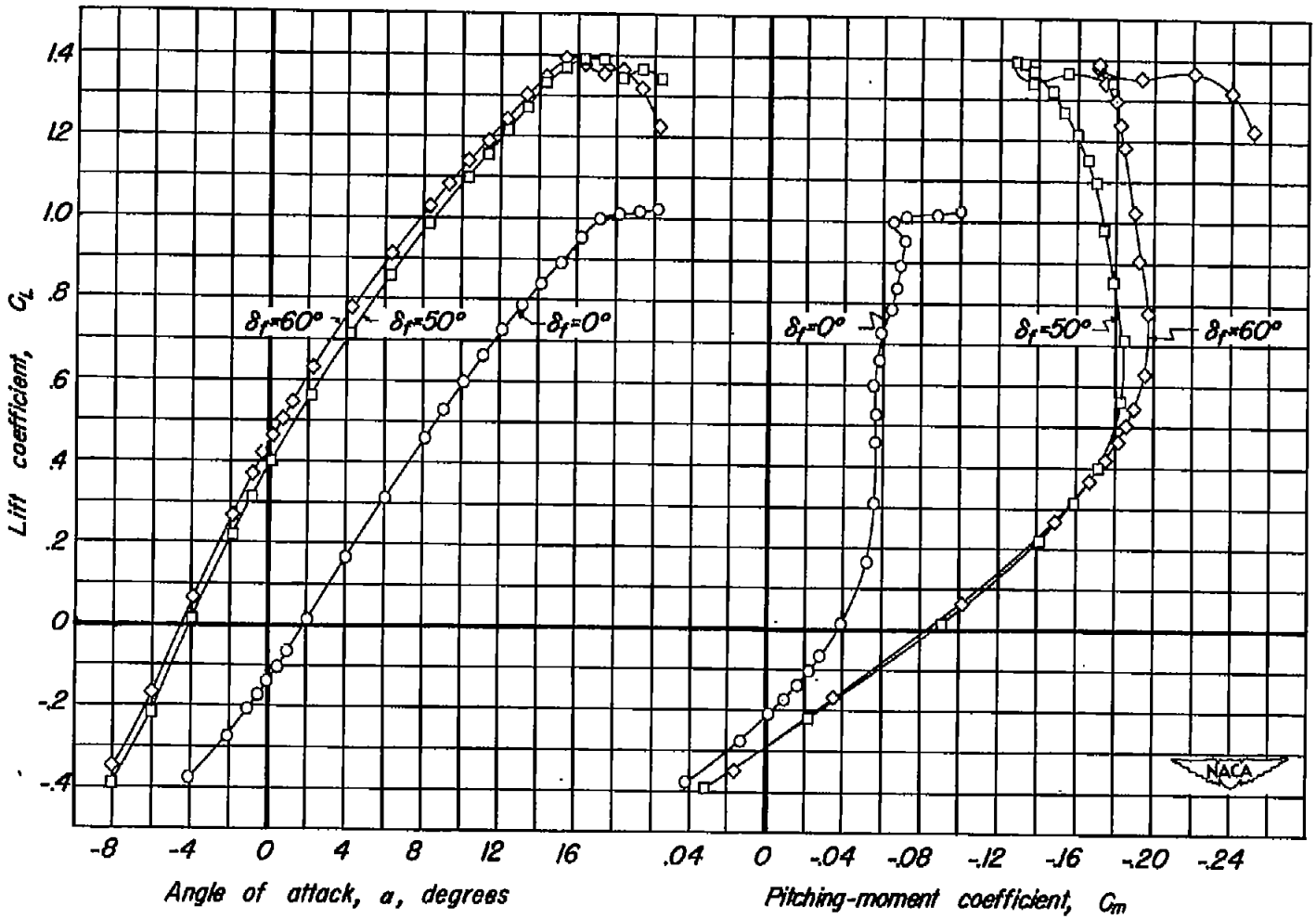

(c) C_L vs α, C_L vs C_m for δ_n = 30°

Figure 6.- Continued.

[redacted]

[redacted]

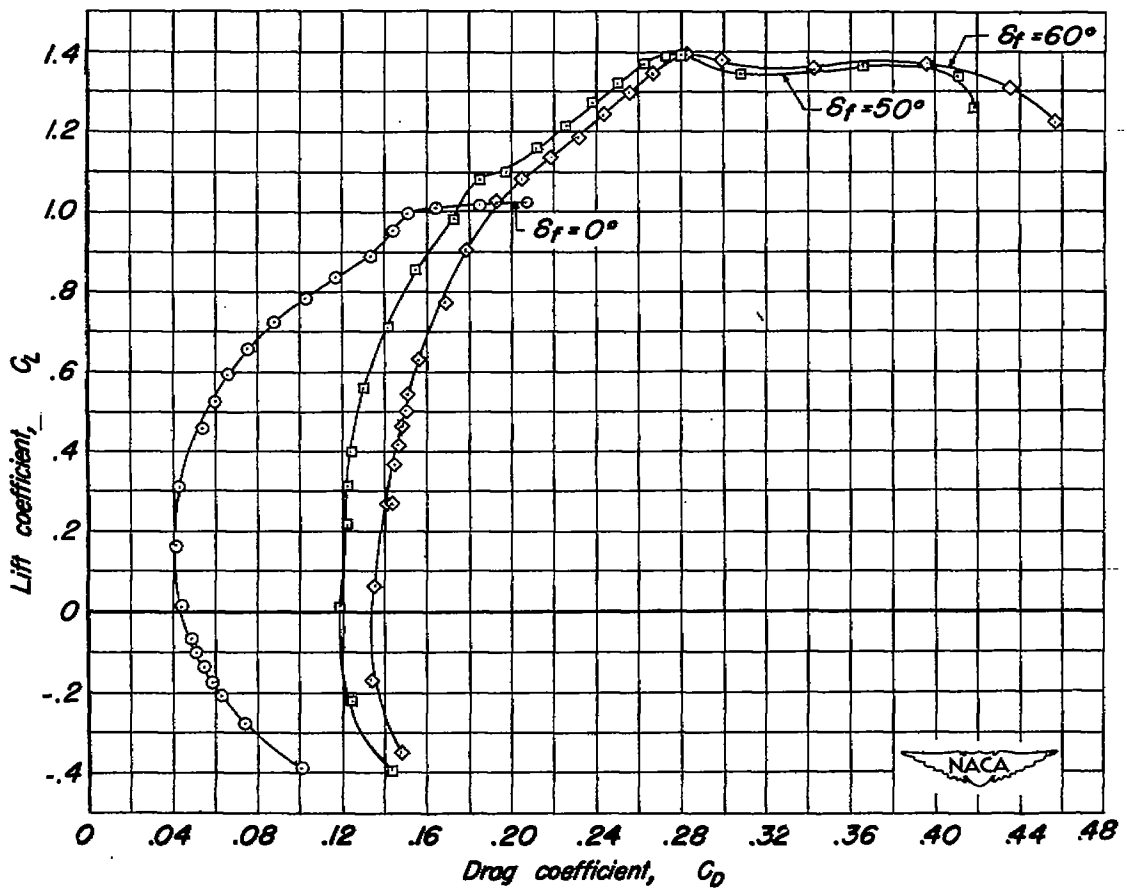

(d) C_L vs C_D for $\delta_n = 30°$

Figure 6.– Continued.

[redacted]

[redacted]

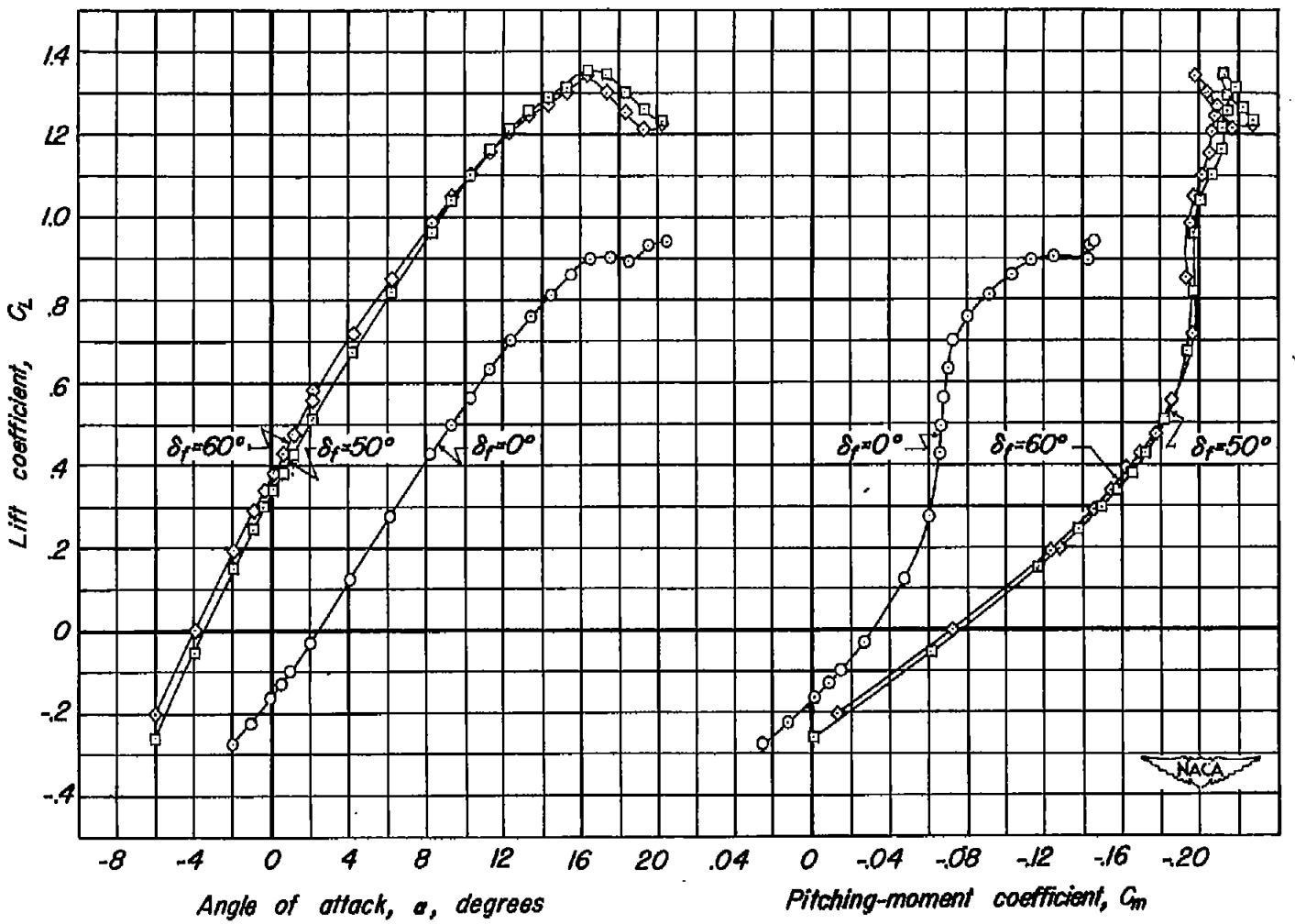

(e) C_L vs α, C_L vs C_m for δ_n=35°.

Figure 6.-Continued.

[redacted]

[redacted]

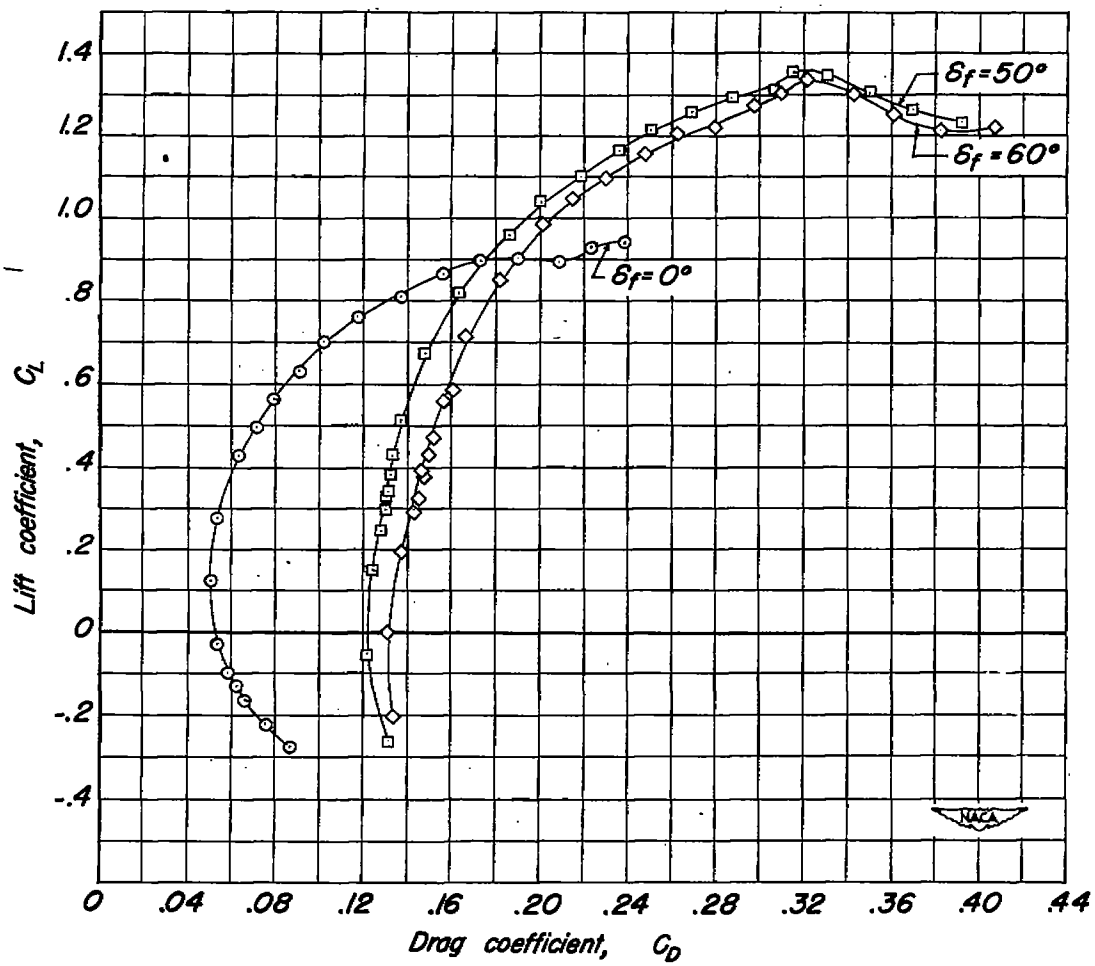

(f) C_L vs C_D for $\delta_n = 35°$.

Figure 6.-Concluded.

[redacted]

[redacted]

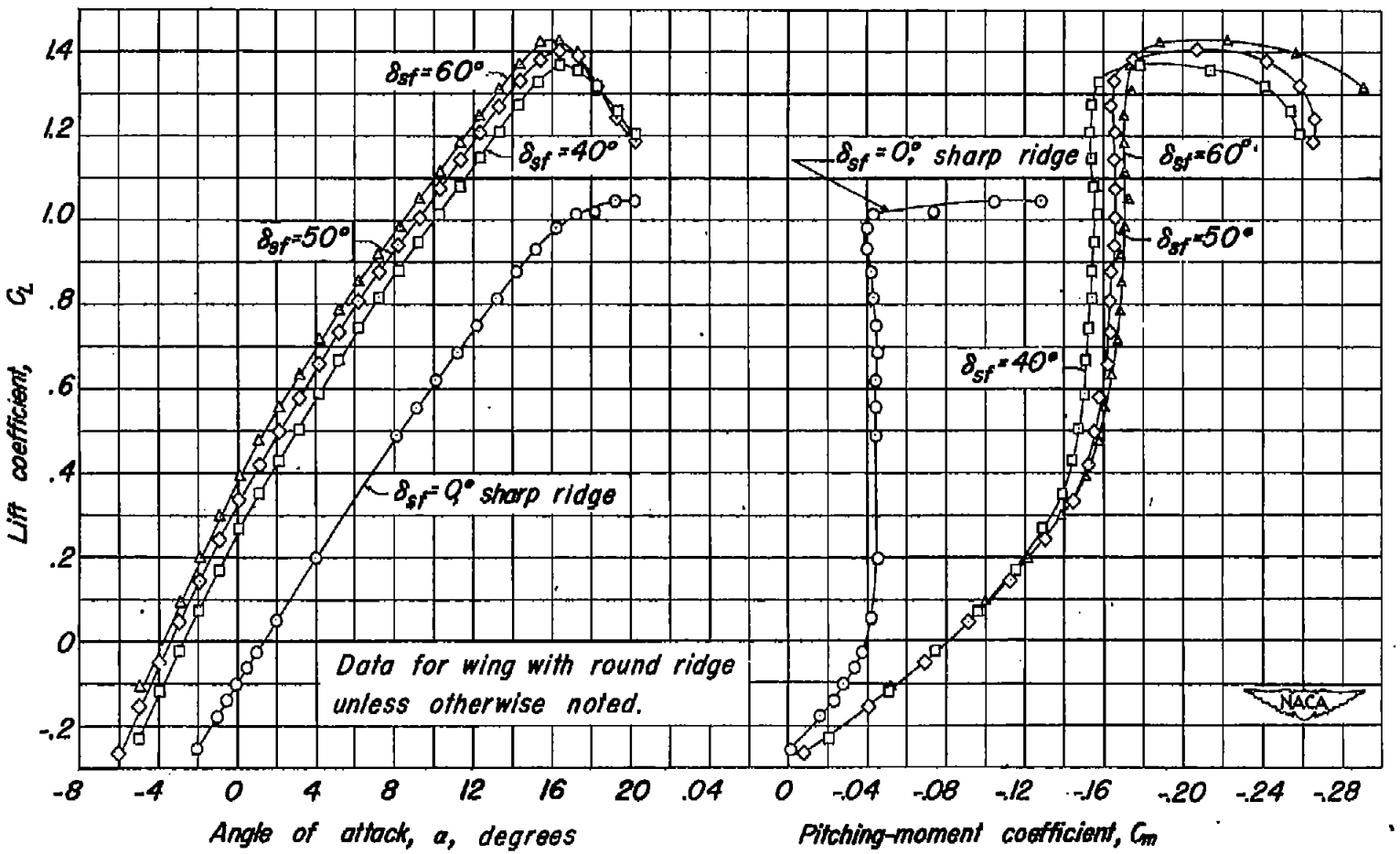

(a) C_L vs α, C_L vs C_m for δ_n=25°.

Figure 7.- The effect of the combination of the leading-edge flap and the trailing-edge split flap on the aerodynamic characteristics of the wing. R,3,000,000; M,0.30.

[redacted]

[redacted]

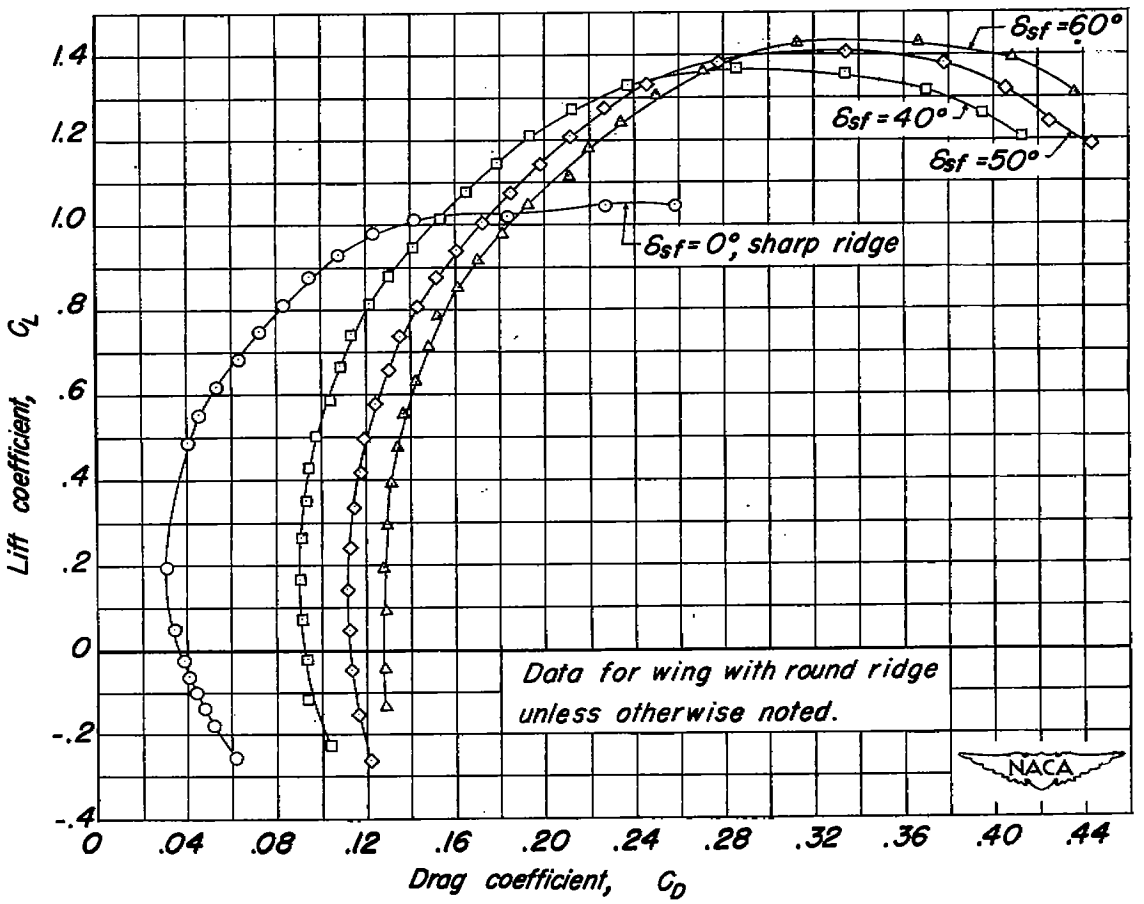

(b) C_L vs C_D for δ_n =25°.

Figure 7.— Continued.

[redacted]

[redacted]

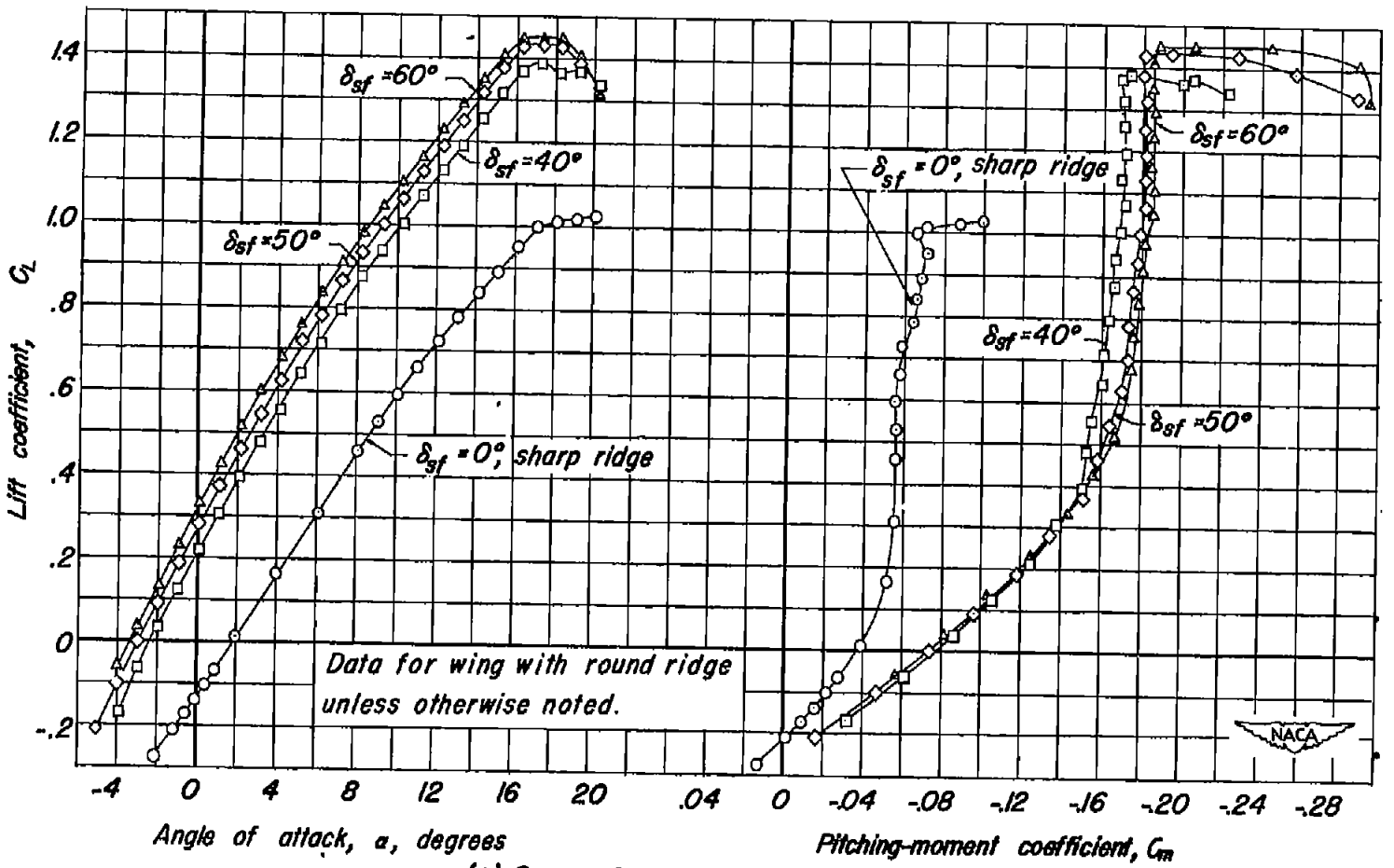

(c) C_L vs α, C_L vs C_m for δ_n =30°.

Figure 7.- Continued.

[redacted]

[redacted]

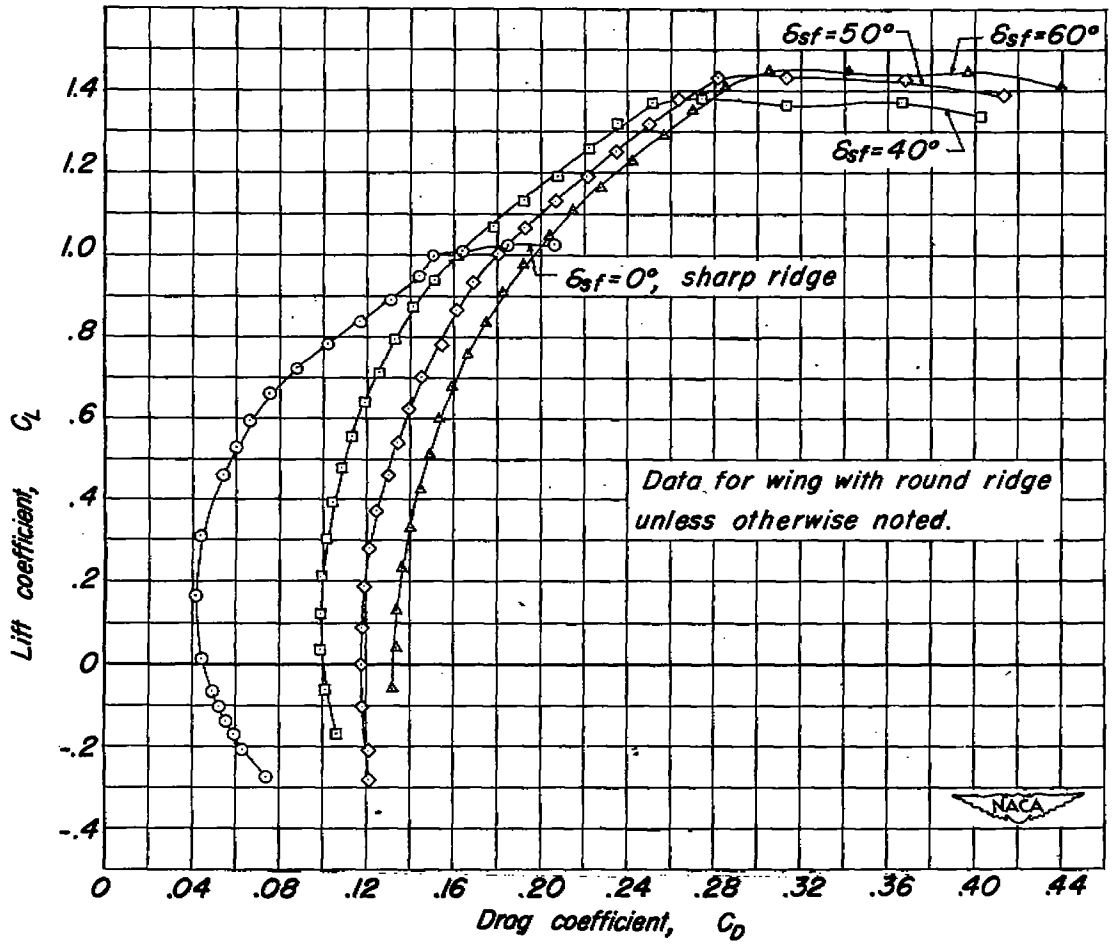

(d) C_L vs C_D for $\delta_n = 30°$.

Figure 7.— Continued.

[redacted]

[redacted]

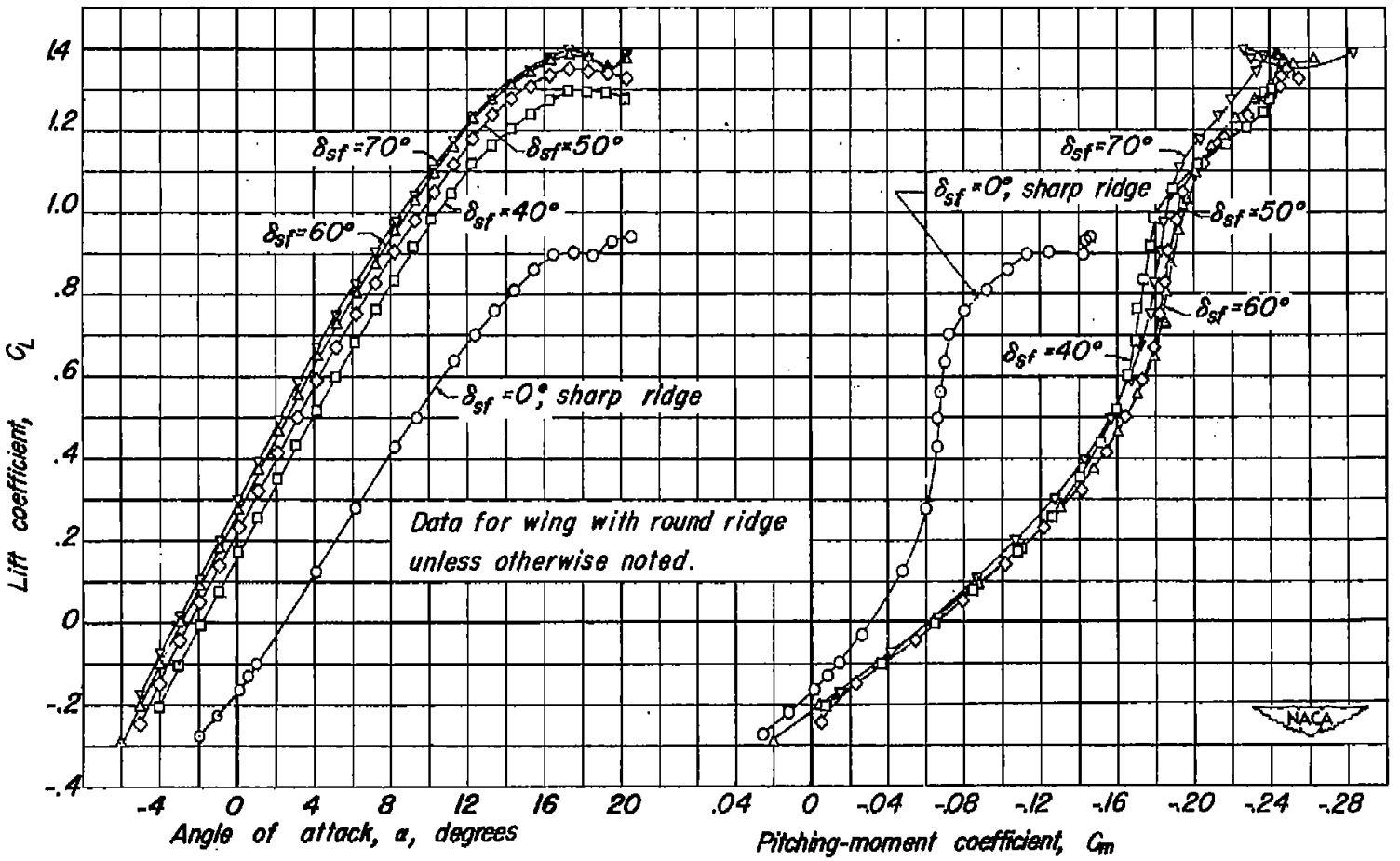

(e) C_L vs α, C_L vs C_m for δ_n=35°.

Figure 7.—Continued.

[redacted]

[redacted]

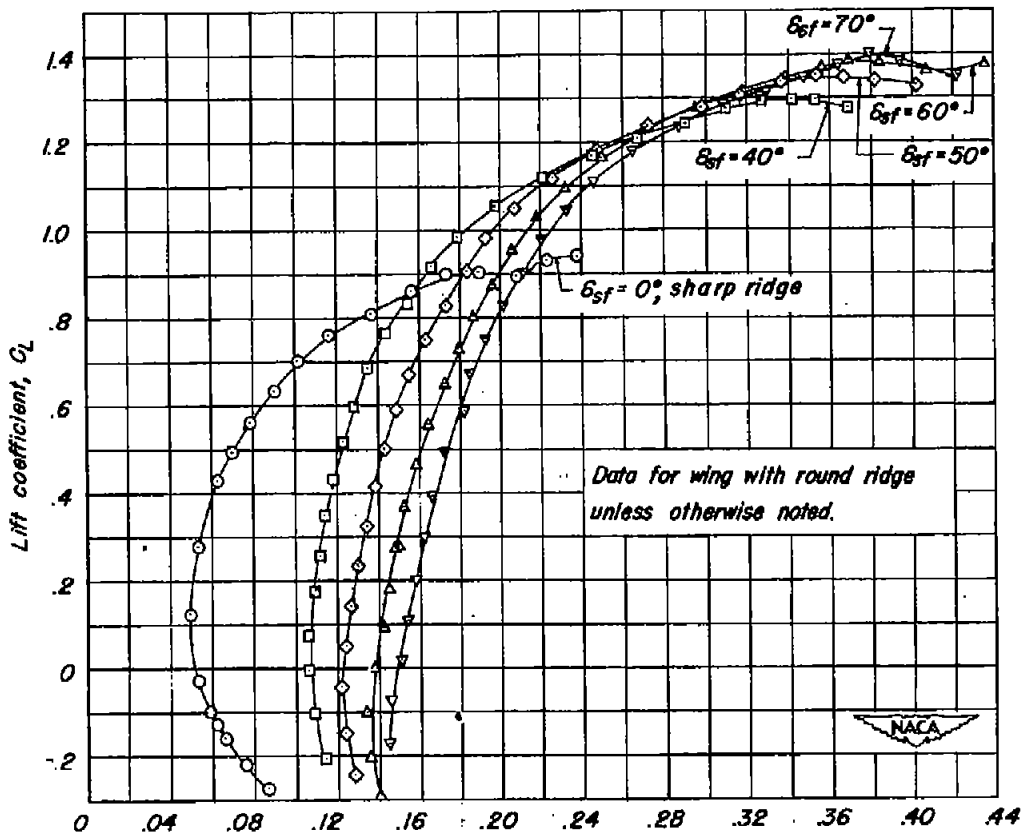

(f) C_L vs C_D for δ_n=35°.

Figure 7.- Concluded.

[redacted]

[redacted]

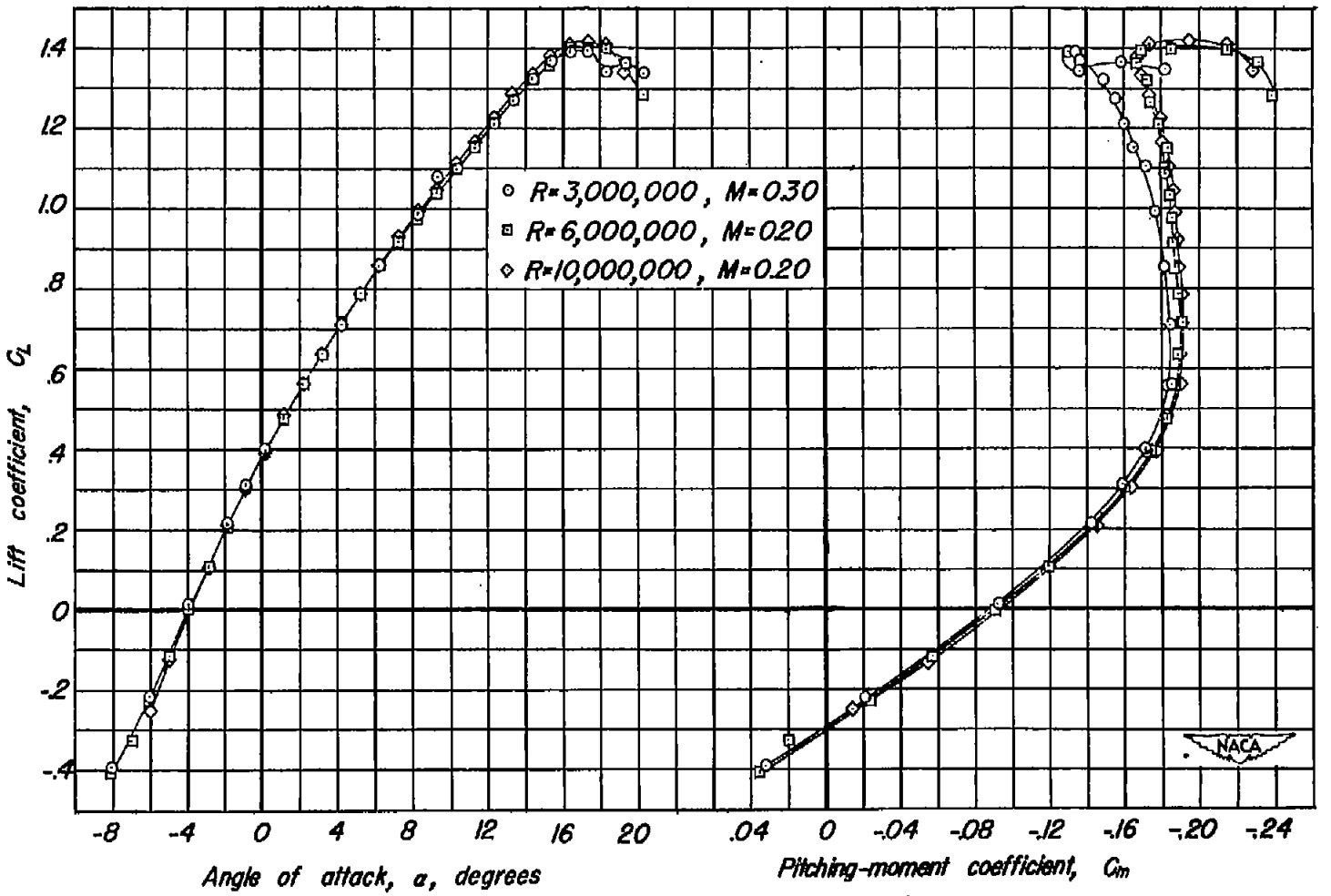

(a) C_L vs α, C_L vs C_m for wing with the sharp-ridge profile.

Figure 8.—The effect of Reynolds number on the aerodynamic characteristics of the wing. δ_n,30°; δ_f,50°.

[redacted]

[redacted]

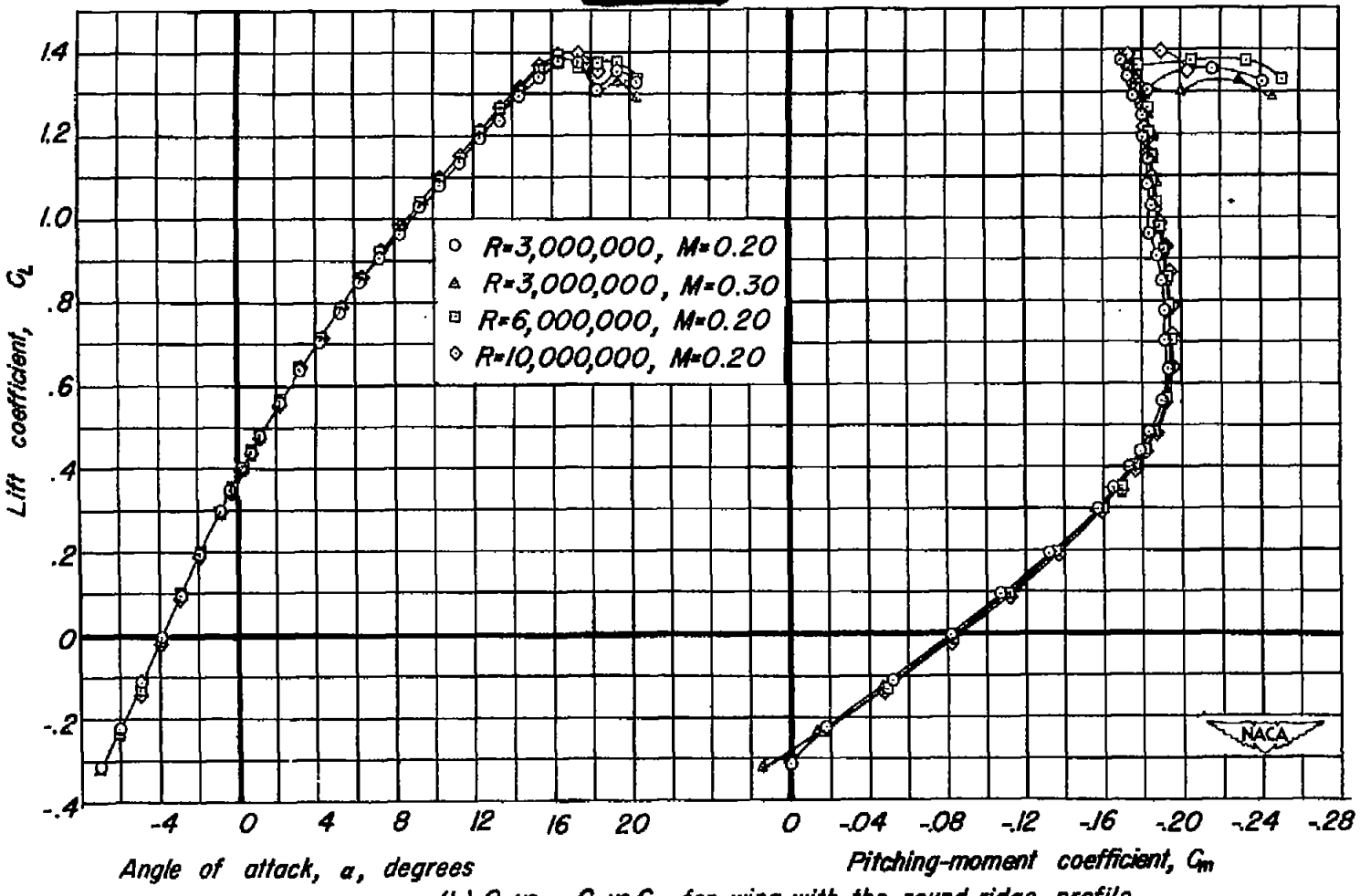

(b) C_L vs α, C_L vs C_m for wing with the round-ridge profile.

Figure 8.—Continued.

[redacted]

[redacted]

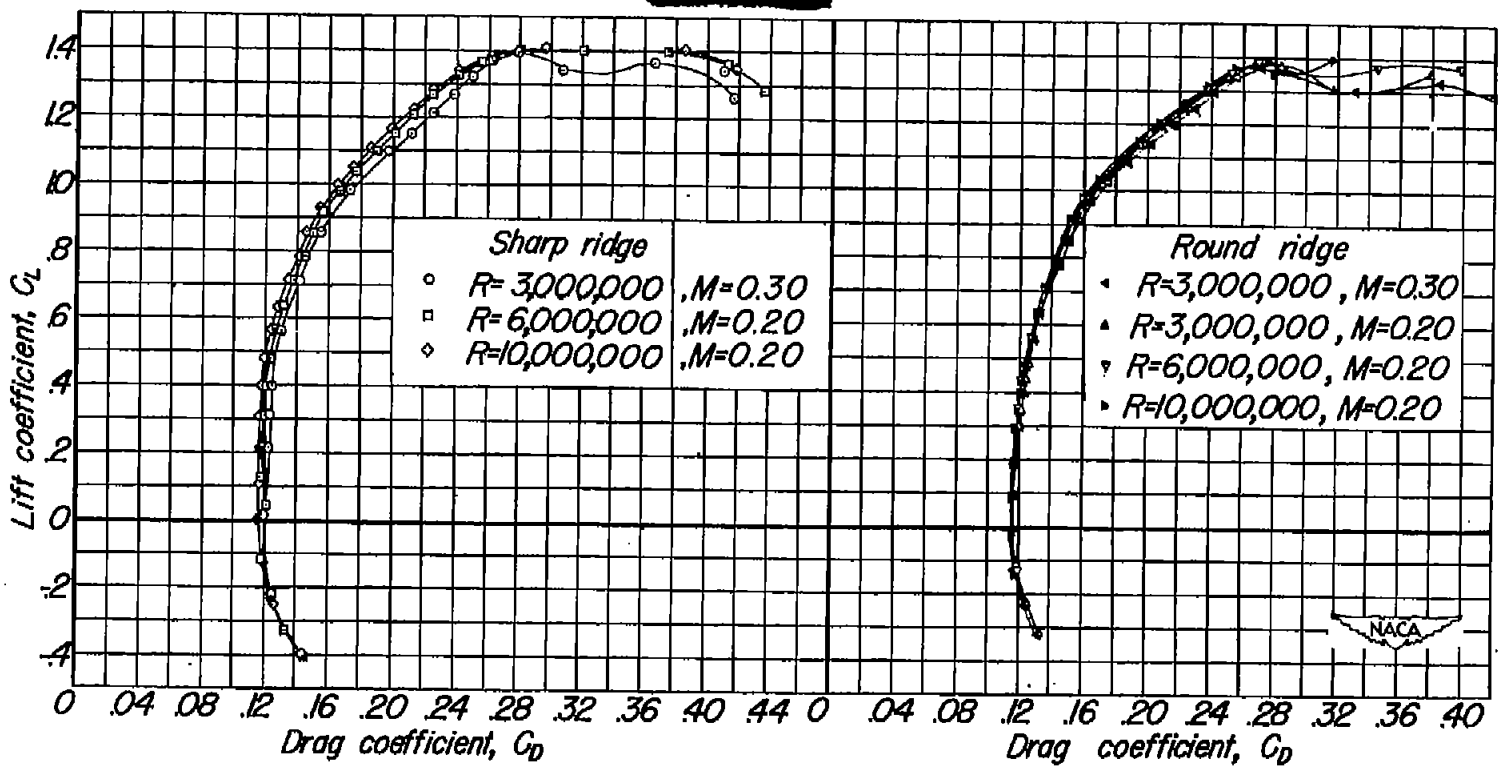

(c) C_L vs C_D.

Figure 8.—Concluded.

[redacted]

[redacted]

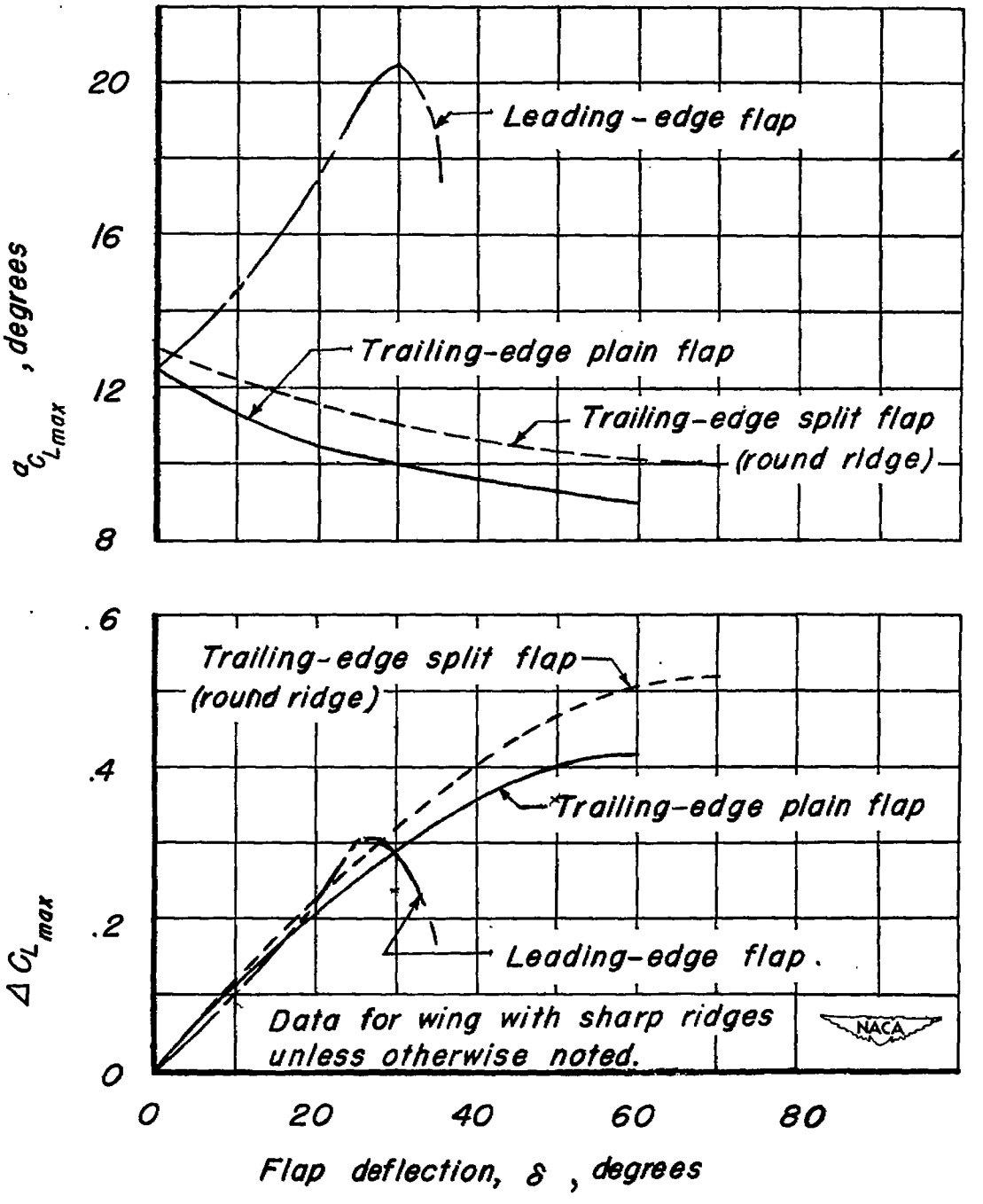

Figure 9.–The effect of flap deflection on the maximum lift characteristics of the wing. R, 3,000,000; M, 0.30.

[redacted]

[redacted]

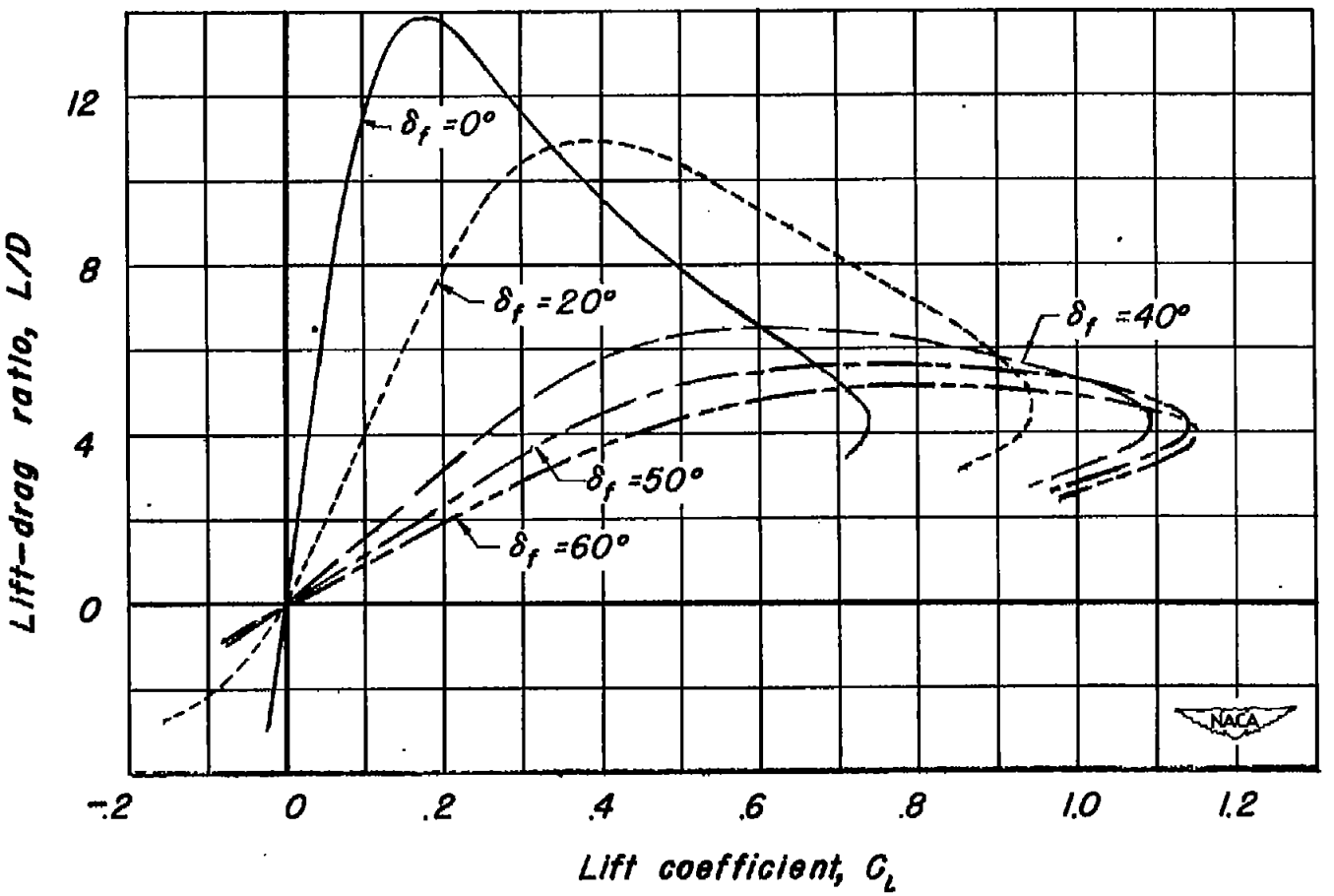

(a) The trailing-edge plain flap ; δ_n ,0° ; sharp-ridge profile.

Figure 10.- The effect of the flaps on the lift-drag ratio. R, 3,000,000; M, 0.30.

[redacted]

[redacted]

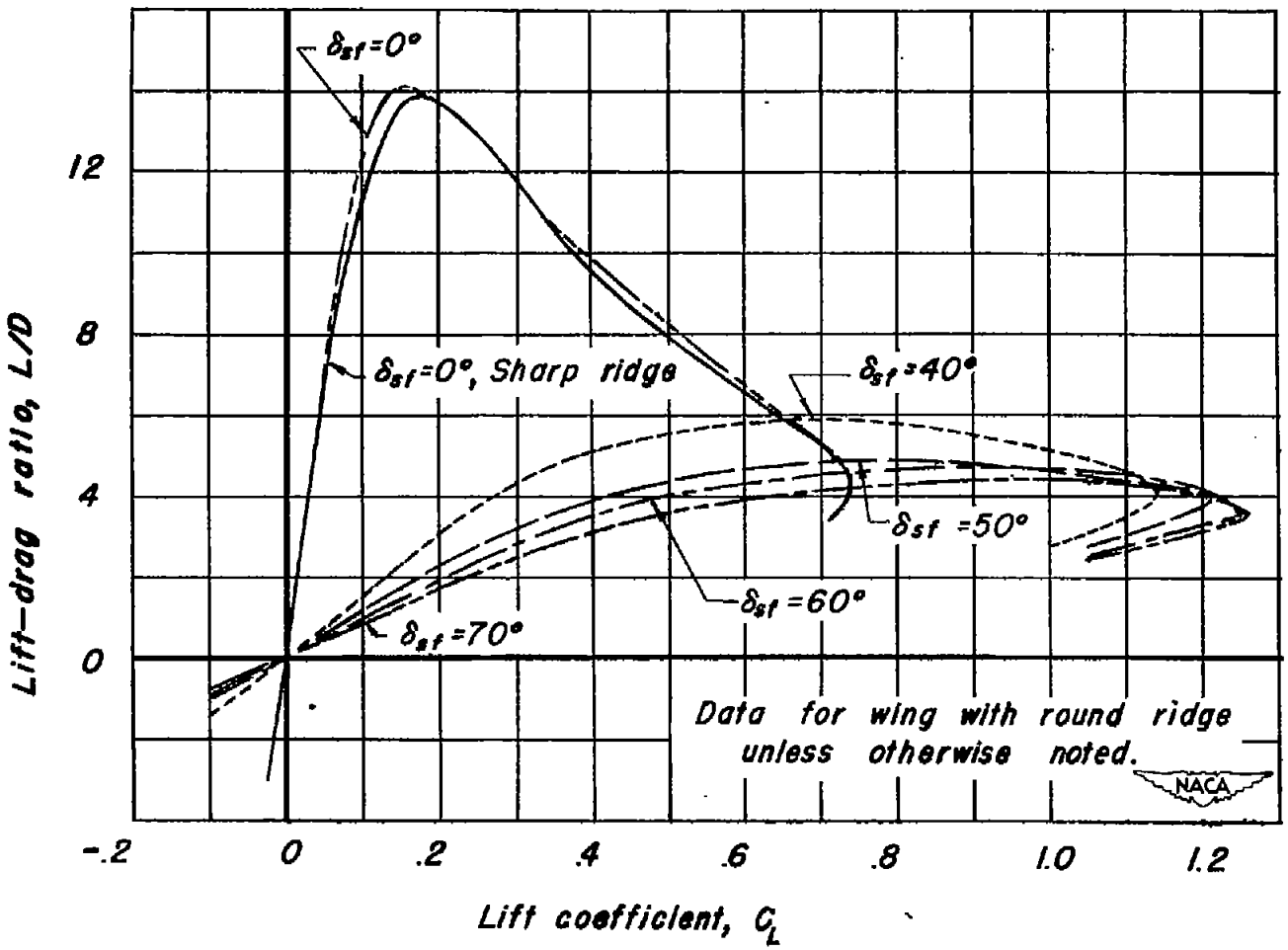

(b) The trailing-edge split flap ; δ_n , 0° .

Figure 10.— Continued.

[redacted]

[redacted]

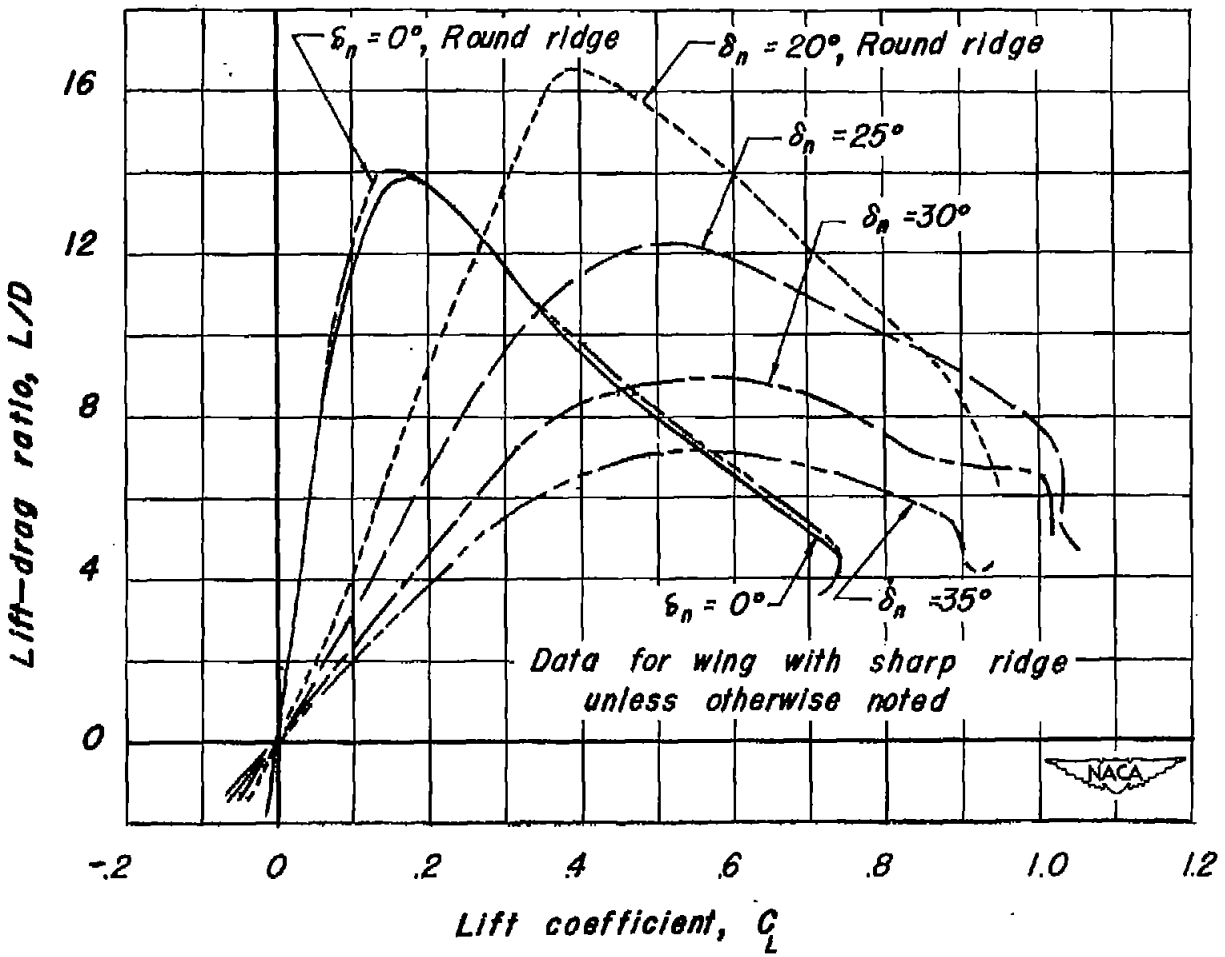

(c) The leading-edge plain flap ; δ_f and δ_{sf}, 0°.

Figure 10.— Continued.

[redacted]

[redacted]

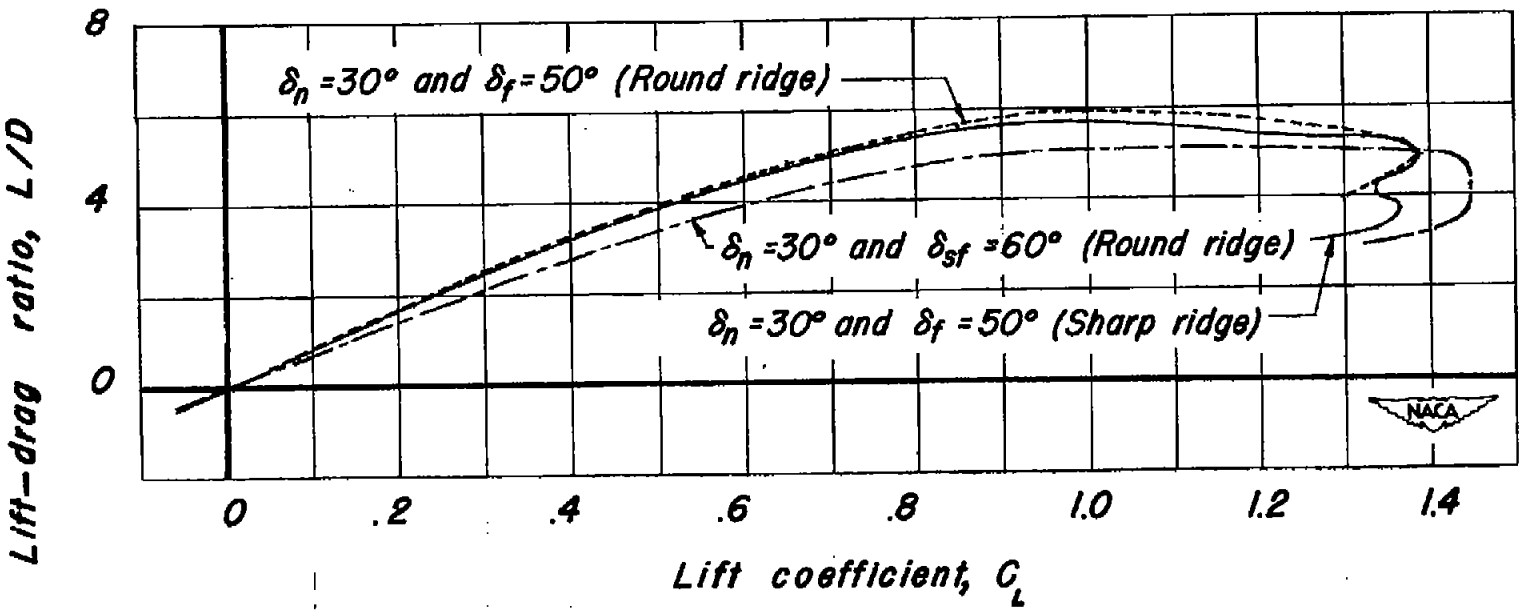

(d) The optimum combinations of the leading-edge flap with the trailing-edge plain flap, and with the trailing-edge split flap.

Figure 10.— Concluded.

[redacted]

LANGLEY RESEARCH CENTER
3 1176 01331 5511